

Overview of the Arctic Sea State and Boundary Layer Physics Program

Jim Thomson¹, Stephen Ackley², Fanny Girard-Ardhuin³, Fabrice Ardhuin³, Alex Babanin¹³, Guillaume Boutin³, John Brozena²³, Sukun Cheng⁸, Clarence Collins⁴, Martin Doble¹⁷, Chris Fairall^{15,16}, Peter Guest²², Claus Gebhardt¹¹, Johannes Gemmrich⁷, Hans C. Graber⁵, Benjamin Holt¹², Susanne Lehner¹¹, Björn Lund⁵, Michael H. Meylan⁶, Ted Maksym²¹, Fabien Montiel¹⁰, Will Perrie¹⁸, Ola Persson^{15,16}, Luc Rainville¹, W. Erick Rogers⁹, Hui Shen¹⁸, Hayley Shen⁸, Vernon Squire¹⁰, Sharon Stammerjohn²⁰, Justin Stopa³, Madison M. Smith¹, Peter Sutherland³, Peter Wadhams¹⁴,

¹Applied Physics Laboratory, University of Washington

²Snow and Ice Geophysics Laboratory, UTSA, San Antonio TX

³Univ. Brest, CNRS, IRD, Ifremer, Laboratoire d'Océanographie Physique et Spatiale (LOPS), IUEM, Brest, France

⁴Coastal and Hydraulics Laboratory, U.S. Army Engineer Research and Development Center, Duck, North Carolina, USA

⁵University of Miami, Center for Southeastern Tropical Advanced Remote Sensing (CSTARS), Miami, Florida, USA

⁶School of Mathematical and Physical Sciences, University of Newcastle, NSW 2308, Australia

⁷Physics and Astronomy, University of Victoria, Victoria, BC, Canada

⁸Clarkson University, Dept. of Civil and Environmental Engineering, Potsdam, NY, USA

⁹Naval Research Laboratory, Stennis Space Center, MS, USA

¹⁰Department of Mathematics and Statistics, University of Otago, Dunedin, New Zealand

¹¹German Aerospace Center (DLR), SAR Oceanography, Bremen, Germany

¹²Jet Propulsion Laboratory, California Institute of Technology

¹³University of Melbourne, Victoria, Australia

¹⁴Cambridge University, Cambridge, UK

¹⁵CIRES/University of Colorado, Boulder, CO, USA

¹⁶National Oceanographic and Atmospheric Administration/Physical Sciences Division, Boulder, CO, USA

¹⁷Polar Scientific, Ltd, UK

¹⁸Fisheries & Oceans Canada and Bedford Institute of Oceanography, Dartmouth, NS, Canada

²⁰Institute of Arctic and Alpine Research, University of Colorado Boulder, Boulder, CO, USA

²¹Woods Hole Oceanographic Institution, Woods Hole, MA, USA

²²Department of Meteorology, Naval Postgraduate School, Monterey CA, USA

²³Code 7420, Marine Geosciences Division, Naval Research Laboratory, USA

Key Points:

- A large study of air-ice-ocean-waves interactions was completed during the autumn of 2015 in the western Arctic.
- Strong wave-ice feedbacks, including pancake ice formation and wave attenuation, were observed.
- Autumn refreezing of the seasonal ice cover is controlled by ocean preconditioning, atmospheric forcing (i.e., on-ice versus off-ice winds), and mixing events.

This is the author manuscript accepted for publication and has undergone full peer review but has not been through the copyediting, typesetting, pagination and proofreading process, which may lead to differences between this version and the Version of Record. Please cite this article as doi: [10.1002/2018JC013766](https://doi.org/10.1002/2018JC013766)

Corresponding author: Jim Thomson, jthomson@apl.uw.edu

Abstract

A large collaborative program has studied the coupled air-ice-ocean-wave processes occurring in the Arctic during the autumn ice advance. The program included a field campaign in the western Arctic during the autumn of 2015, with in situ data collection and both aerial and satellite remote sensing. Many of the analyses have focused on using and improving forecast models. Summarizing and synthesizing the results from a series of separate papers, the overall view is of an Arctic shifting to a more seasonal system. The dramatic increase in open water extent and duration in the autumn means that large surface waves and significant surface heat fluxes are now common. When refreezing finally does occur, it is a highly variable process in space and time. Wind and wave events drive episodic advances and retreats of the ice edge, with associated variations in sea ice formation types (e.g., pancakes, nilas). This variability becomes imprinted on the winter ice cover, which in turn affects the melt season the following year.

1 Introduction

The western Arctic has undergone significant changes in recent decades. Perennial ice cover has been dramatically reduced, and the seasonal ice zone has expanded. This has been widely reported in the literature [e.g., *Jeffries et al.*, 2013; *Wang and Allard*, 2012; *Serreze et al.*, 2016], with many investigations on the consequences of the changing Arctic climate and inter-annual feedbacks [*Maslanik et al.*, 2007]. The Sea State and Boundary Layer Physics of the Emerging Arctic Program sponsored by the Office of Naval Research was designed to examine the specific role of surface waves and winds in the new Arctic, with a focus on the autumn refreezing period. Preliminary results from this program have been reported in *Thomson et al.* [2017] and *Lee and Thomson* [2017]. Here, we link together a series of papers in a special issue detailing many key results from the program.

1.1 Program objectives

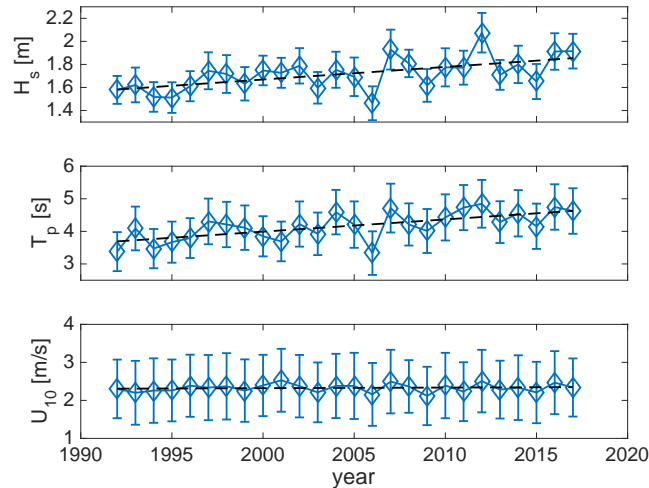
The original objectives of the Arctic Sea State program were described in a science plan [*Thomson et al.*, 2013], as:

- Understanding the changing surface wave and wind climate in the western Arctic,
- Improving numerical and theoretical models of wave-ice interactions,
- Quantifying the fluxes of heat and momentum at the air-ice-ocean interface, and
- Applying the results in coupled forecast models.

Central to the program was a field campaign in the autumn of 2015 aboard the R/V *Siku-liaq*. The data collection was designed to address the objectives above, with a particular focus on data for validation and calibration of process representation in models. These models can then be used both for analysis and forecasting, as well for reanalysis (hind-cast) of the changes occurring in recent decades. The data are also critical for validating new remote sensing techniques which can then provide extensive coverage of waves, ice or ocean parameters.

1.2 Climatology and context

There is a clear trend of increasing surface wave activity in the western Arctic [*Francis et al.*, 2011; *Wang et al.*, 2015; *Liu et al.*, 2016; *Thomson et al.*, 2016; *Stopa et al.*, 2016]. As shown in Figure 1, the increases are both in terms of wave height and wave period. An increase in the wind forcing, however, has not been observed. The signals are consistent with the simple explanation of increasing fetch, because more open water means more room for waves to grow [*Thomson and Rogers*, 2014; *Smith and Thomson*, 2016].



86 **Figure 1.** Trends in the wave heights, wave periods, and wind speeds over the Beaufort and Chukchi seas in
 87 autumn. Updated from [Thomson *et al.*, 2016] with values for 2015, 2016, and 2017. Values are the shape and
 88 scale parameter of Weibull distributions fit to hindcast waves across the months of September, October, and
 89 November.

84 Recently, some investigations have even considered the nearly unlimited fetches that would
 85 occur in an ice-free Arctic [Li, 2016].

90 Coincident with the increasing wave activity from the presence of more open water
 91 is an increase in ocean heating from solar radiation [Perovich *et al.*, 2007]. This is particularly
 92 important during years of early seasonal ice melt, as that may delay refreezing
 93 in the fall [Stroeve *et al.*, 2016]. Stammerjohn *et al.* [2012] have shown that the delay of
 94 autumn refreezing throughout the domain is both a cause and an effect of this increased
 95 ocean heating. The increased heating has led to the seasonal formation of a ‘Near-Surface
 96 Temperature Maximum [NSTM, Jackson *et al.*, 2010] in the upper ocean, which accumulates
 97 heat throughout the open-water season. This ocean heat is either lost (via mixing
 98 and venting to the atmosphere) or trapped (via stratification) when refreezing occurs in
 99 the autumn. The timing of the seasonal refreezing is now delayed a full month later in
 100 the autumn, compared with previous decades [Thomson *et al.*, 2016]. As the timing of
 101 ice refreezing continues to shift, so does the probability of wave activity, given the higher
 102 chance of strong winds in autumn [Pingree-Shippee *et al.*, 2016] that coincide with open
 103 water.

104 **2 Methods**

105 **2.1 In situ observations (R/V Sikuliaq cruise)**

106 The field campaign was a 42-day research cruise on the R/V Sikuliaq, from late
 107 September to early November, 2015. Figure 2 shows the track of the ship, as well as the
 108 ice and wave conditions at end of the campaign. Supplemental material S1 is a movie ver-
 109 sion of this figure, showing the ship position and conditions throughout the entire cruise.
 110 This includes buoy deployments and a count of satellite images acquired.

114 The cruise used a dynamic approach, in which a rolling three-day plan was constantly
 115 updated based on the wind and wave forecast. The primary sampling modules
 116 were:

111 **Figure 2.** Map of cruise track and buoy deployments, overlaid on the ice and wave conditions at the end of
112 the experiment. This is the final frame of a movie, which is included as Supplemental Material S1, showing
113 the progression of the entire research cruise.

- 117 • Wave experiments, in which arrays of up to 17 wave sensing buoys were deployed
118 for hours to days.
- 119 • Ice stations, in which ice floes were surveyed above and below using autonomous
120 systems, and physical samples were collected. Ice Mass Balance (IMB) buoys were
121 also deployed and left for the winter.
- 122 • Flux stations, in which surface fluxes of heat and momentum were measured from
123 the bow of the ship while holding a heading into the wind.
- 124 • Ship surveys, in which an Underway Conductivity-Temperature-Depth (UCTD) was
125 regularly deployed along a track. The ship surveys also include marine X-band
126 radar wave-current-ice observations, visual ice observations, EM ice thickness mea-
127 surements, ice camera recordings, continuous meteorological and flux observations,
128 infrared radiometry, and radiosonde balloon launches.

129 Generally, the wave experiments took precedent whenever there was a favorable forecast
130 for waves, and the other modules fit in around these events. Table 1 in *Cheng et al. [this*
131 *issue]* summarizes the conditions for each wave experiment. The ice stations were selected
132 to span a range of ice types, including multi-year floes. The flux stations were designed
133 to capture both on-ice and off-ice winds over both open water and new ice. The underway
134 surveys provide unique autumn measurements of air-ice-ocean structure and interactions
135 in thin ice and the nearby open water. These include a 'race track' pattern repeated at the
136 shelf break for several days near the end of the cruise. The UCTDs connect the shallow
137 waters of the Chukchi Sea with the deep basin of the Beaufort Sea.

138 **2.2 Remote sensing**

139 Remote sensing was essential for the dynamic approach to the cruise plan. The
140 Sikuliaq received several satellite images daily, mostly from RadarSat2 and TerraSAR-
141 X. These were used to understand the ship's location relative to the sea ice, which often
142 had a complex spatial distribution of multiple ice types and concentrations. In some cases,
143 the images were annotated by analysts from the National Ice Center; these annotations in-
144 cluded probable ice types and predictions of edge changes.

145 Figure 3 shows an example RadarSat2 image with the ship's position on 4 October
146 2017. Supplemental material S2 is a movie of the ice drift at this location, as observed
147 with the ship's radar through a day of working near the ice edge. The ship's radar pro-
148 vided much higher resolution in space and time than the approximately twice daily satel-
149 lite images. *Lund et al [this issue]* apply the ship's radar data to determine ice drift veloc-
150 ity, which can be highly variable. The ship's radar data are also suitable for determining
151 currents and waves [*Lund et al., 2015, 2017*].

152 In addition to the satellite and shipboard systems, two manned aircraft and three un-
153 manned aerial systems (UAS) provided additional data collection and situational aware-
154 ness. The aircraft from the Naval Research Laboratory (NRL) carried LIDAR and L- and
155 P-band SAR, in addition to visual cameras. The aircraft from NASA carried the UVASAR
156 L-band fully polarimetric SAR only (data available at <https://www.asf.alaska.edu/>). The
157 UAS carried visual cameras.

161 In addition to real-time planning, the remote sensing data has also been used for
162 quantitative studies. For example, wind and wave parameters can now be readily derived

158 **Figure 3.** Example RADARSAT-2 image with ship location (green symbol). The orange line is the bound-
159 ary of the US Exclusive Economic Zone (200 nm from the coast). RADARSAT-2 data and products from
160 MacDonald, Dettwiler, and Associates Ltd., All Rights Reserved.

163 from SAR data in the open water [Gemmrich *et al.*, 2016; Gebhardt *et al.*, 2017], and wave
164 heights and full spectra can now be retrieved in ice-covered regions [Arduin *et al.*, 2015;
165 Gebhardt *et al.*, 2016; Arduin *et al.*, 2017]. That method of wave spectra retrieval in ice-
166 covered water was adapted by [Stopa *et al.*, *this issue*] to handle a mixture of wave and ice
167 features, and to estimate the azimuthal cut off that is needed to correct for the blurring of
168 wave patterns near the ice edge. This produced the first map of wave heights extending
169 over 400 km into the ice. The spatial evolution of the wave field in off-ice wind condi-
170 tions is analyzed by [Gemmrich *et al.*, *this issue*]. Other remote sensing data includes ice
171 classification from fully polarized SAR data [Perrie *et al.*, *this issue*], and wave and ice floe
172 mapping from airborne LIDAR data [Sutherland and Gascard, 2016].

173 2.3 Modeling

174 Much of the early effort in the Arctic Sea State program went towards including
175 wave-ice interactions in the operational wave forecast model WAVEWATCH III. Some
176 of the new features were first described in Rogers and Orzech [2013]. These have since
177 been refined and tuned, using the data collected during the Sikuliaq cruise [Rogers *et al.*,
178 2016] and previous datasets [e.g. Arduin *et al.*, 2016]. Prior to these efforts, the only ice
179 scheme available in WAVEWATCH III was to treat as land any regions with ice concen-
180 trations exceeding a fixed threshold [Tolman, 2003], usually at 75%. This early approach
181 did not provide any wave information in the ice, and had a detrimental effect in open wa-
182 ter with a tendency to underestimate wave heights [e.g. Doble and Bidlot, 2013]. The
183 challenge in implementing more physical wave-ice interactions has been the large range
184 in mechanisms and theoretical models proposed for these interactions (see Squire *et al.*
185 [1995] and Squire [2007] for reviews), and the large range of ice types and associated
186 processes. Both wave scattering (conservative) and wave dissipation (non-conservative)
187 actions must be at least considered, although one or the other may dominate in a given
188 set of conditions. Furthermore, each of these processes may be parameterized in various
189 ways: e.g., wave scattering as ‘diffusion’ in Zhao and Shen [2016], or using a scattering
190 matrix which is integrated implicitly [Arduin and Magne, 2007; *The WAVEWATCH III*[®]
191 *Development Group*, 2016].

192 New models have been developed as part of this program [e.g., Montiel *et al.*, 2016],
193 and thus there is an expanding set of schemes to implement and test in WAVEWATCH
194 III. These are noted by ‘ICn’ for dissipation terms and ‘ISn’ for scattering terms. Recent
195 developments are documented in the WAVEWATCH III manual [*The WAVEWATCH III*[®]
196 *Development Group*, 2016] and in Collins and Rogers [2017] for IC4, including a calibra-
197 tion study for the Sikuliaq cruise. Additional efforts include Boutin *et al.* [*this issue*] and
198 Arduin *et al.* [*this issue*] with effects on ice break-up on IC2 and IS2, and implementa-
199 tion of the “extended Fox and Squire” model (Mosig *et al.* [2015]) in WAVEWATCH III
200 as IC5. The various schemes are summarized in Table 1. Collins *et al.* [2017a] explore
201 the changes in the wave dispersion relation from various physical models, and Mosig *et al.*
202 [2015] compare several viscoelastic models. Li *et al.* [2015a] explore the sensitivities of a
203 particular viscoelastic model.

Table 1. Wave-ice interaction schemes in WAVEWATCH III.

| Scheme | Mechanism |
|--------|--|
| IC0 | Partial blocking, scaled by ice concentration; high concentration treated as land |
| IS1 | Simple conservative diffusive scattering term |
| IS2 | Floe-size dependent conservative scattering, combined with ice break-up, and anelastic and/or inelastic dissipation due to ice flexure |
| IC1 | Simple dissipation, uniform in frequency |
| IC2 | Basal friction, laminar and/or turbulent |
| IC3 | Ice as viscoelastic layer [Wang and Shen, 2010], frequency-dependent |
| IC4 | Assorted parametric and empirical formulae, most being frequency-dependent |
| IC5 | Ice as viscoelastic layer [extended from Fox and Squire, 1994], frequency-dependent |

3 Results

3.1 Atmospheric forcing

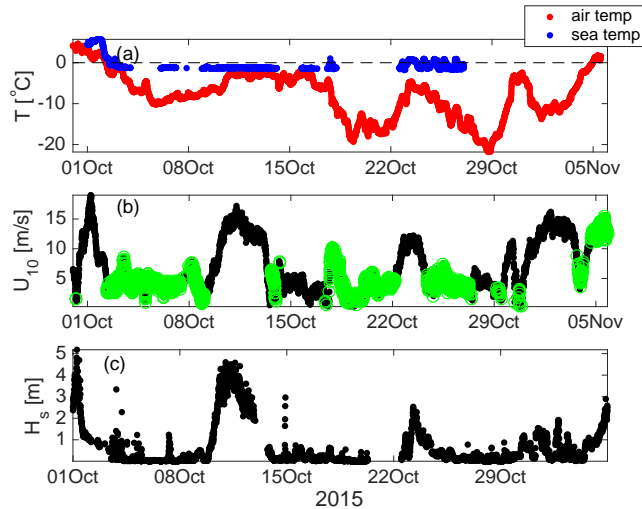
Much of the autumn ice advance is driven by the atmospheric forcing. Figure 4 shows the conditions throughout the cruise, as measured by instruments on the ship. The air was cold enough for freezing conditions throughout almost the entire cruise, but it is the full surface energy budget that controls freezing, not just sensible heat flux. The most significant influence on air temperature is the wind direction; much colder temperatures are associated with off-ice winds. Under such conditions, the lower atmosphere is cooler over the ice, producing cold-air advection by the off-ice winds over the nearby open water. The very cold, dry air can cause rapid cooling and freezing at the ocean surface [Persson *et al*, *this issue*]. By contrast, on-ice winds can carry relative warm air from over the ocean. In either case, the gradients between these air masses can form strong low-level jets along the ice edge [Guest *et al*, *this issue*].

On-ice winds can drive significant upper ocean mixing that may delay freezing or even cause a temporary reversal of the autumn ice advance. Smith *et al* [*this issue*] explore one such mixing event (Wave Experiment 3, 10-13 October 2015) in great detail. Figure 5 shows example images of the surface, along with the surface forcing and fluxes. The upper image is at the beginning of the event, when frazil ice is forming, and the lower image is at the end, when the frazil ice has become pancakes and upper ocean heat released due to mixing is melting the pancakes.

While Figure 4 shows a strong correlation between wind speed and wave height (as expected), the details are obscured since the ship position varied between being in the ice, at the ice edge, or in open water during different events. Wind stress is essential both for wave growth and for momentum transfer into the ocean, and the relation of wind speed to wind stress in this environment is often sensitive to the combined ice and wave conditions. For practical purposes, this is parameterized with a drag coefficient. Determination of the drag coefficient at the air-sea-ice boundary is critical to accurate atmospheric forcing [Martin *et al.*, 2016] and to wave modeling [Tolman and Chalikov, 1996].

3.2 Waves

Waves were observed using freely drifting buoys during seven wave experiments (see Table 1 in Cheng *et al* [*this issue*]). Waves were also observed along the ship track using a LIDAR range finder mounted at the bow, for which the measurements have been Doppler corrected according to Collins *et al.* [2017b], and the ship's radar. The maximum waves observed were almost 5 m significant wave height on 12 October 2017, in the middle of Wave Experiment 3 (see Figure 4). This is the upper end of the climatology determined



225 **Figure 4.** Time series of basic parameters along the cruise track: air and ocean temperatures (a), wind
 226 speeds (b), and wave heights (c). The green circles in (b) indicate the off-ice wind conditions. Red circles and
 227 blue circles in (a) refer to air and sea temperatures, respectively.

236 **Figure 5.** Example surface conditions and associated parameters during Wave Experiment 3 (10-12 Octo-
 237 ber 2015).

256 **Figure 6.** Scaled histogram of observed in situ wave heights during the Sikuliaq cruise (black dots), com-
 257 pared with Weibull distributions of the hindcast wave heights throughout the domain for October of the years
 258 2007 through 2014 (colored curves). Hindcast from Thomson *et al.* [2016].

259 **Figure 7.** Histogram of wave heights observed remotely using the TerraSAR-X satellite system during
 260 October 2015.

245 by Thomson *et al.* [2016] for the previous two decades. Figure 6 compares the distribution
 246 of wave heights from in situ wave observations during all wave experiments to the clima-
 247 tology distributions. Figure 7 shows a similar distribution of wave observations using the
 248 TerraSAR-X satellite system. The observations have peaks well above the climatology, be-
 249 cause the adaptive sampling was targeting events with large waves. The in situ distribution
 250 (Figure 6), in particular, has a local minimum between 1 and 2 m wave heights, which
 251 is likely related to having very few samples out in open water absent a big wave event.
 252 (Wave heights of 1-2 m are now typical in the open water areas of the western Arctic.)
 253 Although these distributions reveal some sampling biases, it was not the intent to observe
 254 the climatology; the intent was to observe processes, especially those that are tied to wave-
 255 ice interactions with an increasing sea state climatology.

261 The full suite of wave observations have been used to determine attenuation of waves
 262 in pancake ice and then calibrate a viscoelastic model [Cheng *et al.*, *this issue*]. This is the
 263 IC3 wave-ice scheme from Table 1, and the results suggest that elasticity is of less impor-
 264 tance than the viscous damping. This is a consequence of pancake ice being much smaller
 265 than the wavelength; scattering is not expected to be important in this regime. Stopa *et al*
 266 [this issue] have also determined attenuation further into the ice pack during Wave Ex-

267 periment 3, using a larger domain thanks to wave heights derived from Sentinel 1 SAR
268 imagery. The associated processes appear very different from what is found in pancake
269 ice and is described by *Boutin et al [this issue]* and discussed by *Ardhuin et al [this issue]*.
270 *Montiel and Squire [this issue]* further analyze wave attenuation and directional spreading
271 during the large wave event of Wave Experiment 3. A key finding is that waves may tend
272 to attenuate linearly for large amplitudes and exponentially for small amplitudes, mirroring
273 the observations of *Kohout et al. [2014]* in the Antarctic MIZ.

274 *Meylan et al [this issue]* analyzed the power law dependence of attenuation on fre-
275 quency for both measurements and models. The measurements showed universal power
276 law dependence, being approximately four for pancake/frazil ice and two for large floes.
277 While the models for attenuation generally have free parameters, their dependence as a
278 function of frequency is fixed. Currently we do not know the mechanism for the energy
279 loss. *Meylan et al [this issue]* also show how we can connect the energy loss mechanism
280 to the power law dependence.

281 A consistent result from all of these approaches is that attenuation is frequency de-
282 pendent, with the strongest effects at the high frequencies. This general effect has been
283 observed in numerous prior experiments [e.g., *Collins et al., 2015; Wadhams et al., 1988*].
284 Data from the Sea State project provide opportunities to further quantify the low-pass
285 filtering nature of different first-year ice types. Supplemental material S3 is a video of
286 waves in pancake ice, in which the suppression of high frequency waves is visually appar-
287 ent.

288 One specific issue from previous studies has been the apparent “roll-over” of atten-
289 uation at the very highest frequencies. The analyses of *Rogers et al. [2016]* did not find a
290 roll-over for the Wave Experiment 3 and those authors speculate that cases of roll-over re-
291 ported in some prior studies were spurious outcomes resulting from regeneration of wave
292 energy by wind. Likewise, *Li et al. [2015b]* suggested that the linear rather than exponen-
293 tial attenuation at large wave amplitude reported for a case in Antarctic MIZ in *Kohout*
294 *et al. [2014]* might also be partly due to this wind input. Most recently, *Li et al. [2017]*
295 confirmed that roll-over in the same Antarctic case likely is a result of wind input to the
296 highest frequencies. The wind input causes it to appear that less attenuation occurred,
297 when comparing the net difference between two measurements (i.e., two buoys). In real-
298 ity, the attenuation continues to increase with frequency. Though the above are specific
299 case studies and results cannot be conclusively generalized to all prior wave-in-ice studies,
300 one conclusion is unambiguous: in cases where local wind is not small, wind input *must*
301 *be included* to obtain correct estimates of attenuation of wave energy by sea ice, and this
302 is particularly crucial for estimates of the frequency-dependence of this dissipation.

303 *Wadhams et al. [this issue]* use spectra of satellite SAR images to infer attenuation
304 and invert for pancake ice thickness. *Brozana and Sutherland [this issue]* determine atten-
305 uation rates from the airborne LIDAR and examine the importance of scattering, relative
306 to dissipation. *Collins et al [this issue]* evaluate changes in the dispersion relation and con-
307 clude that they are small and confined to the higher wave frequencies where the wavenum-
308 ber tends to increase relative to open water. This suggests, as expected, that elasticity is
309 not important in the MIZ.

310 In addition to wave attenuation, wave growth is also studied with this dataset. Fol-
311 lowing *Gebhardt et al. [2017]*, *Gemmrich et al. [this issue]* use TerraSAR-X wave esti-
312 mates to examine fetch-limited growth of waves during off-ice wind conditions. They
313 find mostly conventional fetch laws, with only limited evidence that waves experience any
314 growth in partial ice cover. This is consistent with the very small wind input rates deter-
315 mined by *Zippel and Thomson [2016]* in partial ice cover.

317 **Figure 8.** Ice type distribution along the ship track and sample photos of each type. The size of the circles
318 in the distribution represents the partial concentration of each type.

342 **Figure 9.** Example of multi-year ice (MYI) sampled on 6 October 2015 using UAVASAR (a,b), marine
343 radar (c), and physical sampling (d).

345 **Figure 10.** Sea surface temperature anomaly (colors, derived from SST data available at
346 <https://mur.jpl.nasa.gov>) and ice cover (grayscale, derived from AMSR2, data available at [https://seaice.uni-](https://seaice.uni-bremen.de/start/data-archive)
347 [bremen.de/start/data-archive](https://seaice.uni-bremen.de/start/data-archive)) in the western Arctic at the start of Sikuliaq research cruise (magenta is track
348 line).

316 3.3 Sea Ice

319 Hourly ice observations from the bridge of the ship, using the ASSIST protocols,
320 show a wide variety of ice types and concentrations. Figure 8 shows the distribution of
321 three dominant ice types along the cruise track. Two types are particularly common: pan-
322 cake ice and nilas ice (the latter is shown as "Other " in Figure 8). These form in wavy
323 and calm conditions, respectively. As discussed in *Thomson et al.* [2017], the observation
324 of extensive pancake ice in the western Arctic is quite novel, and it is clearly an effect of
325 the increasing wave climate. These ASSIST observations are complemented by a data set
326 of shipboard images; examples are Figure 8.

327 *Roach et al. [this issue]* examine the lateral growth and welding of pancakes us-
328 ing in situ data, and find both processes are negatively correlated with significant wave
329 height. The tensile stress arising from the wave field exerts a strong control on pancake
330 size. They also evaluate lateral growth and welding predicted by parametrization schemes,
331 which can be used to inform development of state-of-the-art sea ice models. *Lund et al*
332 *[this issue]* quantify the ice drift motions, in particular the relation to the wind and the
333 advection by ocean currents. Several studies look at the ice thickness evolution. As men-
334 tioned above, *Wadhams et al [this issue]* do this from satellite data. *Persson et al [in prep]*
335 use a thermodynamic estimate, based on the difference between the skin temperature and
336 the sub-surface temperature. In addition, observations of sea ice deformation features were
337 made at six locations using an autonomous underwater vehicle, and a suite of buoys were
338 deployed on the ice to track ice development as the fall progressed.

339 The program also observed multi-year floes, including the study by *Ackley et al [this*
340 *issue]* which uses isotopes to understand the relative importance of snow melt and seawater,
341 especially in melt ponds. An example of multi-year ice is shown in Figure 9.

344 3.4 Ocean

349 The western Arctic Ocean in autumn has absorbed a significant amount of heat in
350 the preceding months. This signal however, can be very spatially heterogeneous. In 2015,
351 a remnant tongue of ice persisted in the Beaufort Sea throughout much of the summer,
352 and this created a region of cooler sea surface temperature in the autumn (Figure 10).
353 This preconditioning likely influenced the progression to refreezing. Following along the
354 ship track, significant variations in ocean heat content were observed. *Smith et al [this is-*
355 *sue]* study the strong on-ice wind event of Wave Experiment 3 (10-13 October 2015) and
356 show that release of stored ocean heat is sufficient to cause a temporary reversal of the au-
357 tumn ice advance. Later in the cruise, the ocean heat content was particularly varied near

386 **Figure 11.** Wave height time series during Wave Experiment 3. Black dots are observations from the
387 NIWA buoy. Colored dots are from a WAVEWATCH III hindcast using the original ice parameterization
388 (green) and newly implemented ice parameterizations (red, blue).

399 **Figure 12.** Mean Arctic ice cover in the late 20th century (left columns) and predicted for the late 21st
400 century (right columns) for the months of August, September, and October.

358 the shelf-break, where the advancing ice edge appeared to loiter, analogous to loitering of
359 the retreating ice edge in the spring [Steele and Ermold, 2015]. This loitering was only
360 disturbed by very strong cooling coincident with off-ice winds *Persson et al [this issue]*.

361 4 Discussion

362 4.1 Forecast challenges

363 Forecasting was crucial to the research cruise, because the timing and location of
364 the wave experiments were planned in near real-time. The forecasts available on the ship
365 were a combination of operational products and custom products developed as part of the
366 larger research program. At the time of the Sikuliaq cruise, most models used only one-
367 way coupling (or no coupling). For wave forecasting, this meant that the sea ice model
368 was simply an input to the wave model, and the waves could not feedback to the ice. In
369 many cases, the sensitivity to the quality (or lack) of the ice input was severe.

370 In a hindcast analysis, such as the wave height time series in Figure 11, the wave
371 model can be tuned and the ice input selected to achieve good agreement with in situ
372 wave observations. A priori, however, it can be very difficult to know which ice param-
373 eterization to choose and which ice input to use. This is further complicated by the dis-
374 crepancies between ice models and ice observations (see Figures S6, S7 of *Cheng et al.*
375 [2017]). Clearly, the new parameterizations (ICn) are superior to the original one (IC0),
376 but there are still significant differences among the parameterizations (see Figure 11). In
377 particular, the different parameterizations can have very different performance in replicat-
378 ing the spectral filtering that is often observed in ice, in which high-frequency components
379 are attenuated and low-frequency components propagate unaltered. Further complicating
380 the matter is that model results from WAVEWATCH III are sensitive to all source terms,
381 not just ice, and these other source terms, in particular wind input and nonlinear inter-
382 actions, may also change in the presence of ice. These source terms have been tuned in
383 open water conditions only. Inter-dependence of these source terms has been indicated in
384 *Cheng et al. [2017]*. This effect is obscured when examining wave heights alone, but can
385 be crucial to questions of mixing [*Smith et al, this issue*].

389 4.2 Feedbacks and future climate scenarios

390 The challenge in creating models capable of forecast and climate predictions is in
391 the highly coupled nature of the air-sea-ice-wave processes [e.g., *Khon et al., 2014*]. Al-
392 though this program has produced many improvements in fundamental understanding of
393 the coupled processes and the model representation thereof, there is still a strong need to
394 develop better model coupling. The need is urgent, given the scenarios for extreme change
395 in the Arctic. Figure 12 compares historical ice cover with the CIOM A1B scenario pre-
396 dictions for the end of this century [*Long and Perrie, 2013, 2015, 2017*]. The ice-free Au-
397 gust is remarkable, but the October ice cover is more so because it implicates all of the
398 processes explored in this program.

401 For example, pancake formation, or almost any ice type, is not included in ice mod-
402 els. This would almost surely involve coupling to a wave model. There is recent progress
403 in representing the wave-forced breakup of ice into specific Floe Size Distributions [FSD,
404 *Montiel and Squire, 2017*], that has yet to be included in any wave-ice model. A comple-
405 mentary avenue for progress in this area is in laboratory experiments, where interacting
406 processes may be isolated. For example, details of the wave interactions with individual
407 ice floes is more readily apparent [*Bennetts et al., 2015*].

408 Similarly, the details of wave and wind coupling in the presence of ice are not fully
409 understood. Although wind input is reduced in ice [*Zippel and Thomson, 2016*], there may
410 still be sufficient wind input to offset some of the attenuation [*Li et al., 2015b, 2017*].

411 The recent trend of decreasing ice cover in the fall in the Chukchi/Beaufort region
412 exposes the relatively warm ocean surface to the atmosphere, causing deeper and more
413 unstable atmospheric boundary layers, which results in higher winds, wind stress and tur-
414 bulent heat fluxes at the surface. Also the presence of ice edges and marginal ice zones
415 (which only existed to the south in previous decades) creates horizontal temperature gra-
416 dients that can create low level wind jets, several of which were experienced during the
417 cruise [*Guest et al., this issue; Persson et al, this issue*]. More open water will likely result
418 in generation of previously-rare mesoscale cyclones, including Polar Lows [*Inoue et al.,*
419 *2010*], and also may result in changes to synoptic-scale cyclone storm tracks, bringing
420 more storms into the region [*Wang et al., 2017*]. These phenomena indicate the impor-
421 tance of considering atmospheric feedbacks in understanding air-ice-ocean interaction and
422 wave generation in the Arctic.

423 5 Conclusions

424 The Arctic Sea State program has quantified the trend of increasing waves in the
425 western Arctic and the implications for air-ice-ocean processes. In 2013 when the sci-
426 ence plan of the Sea State program was written, it was only a conjecture that waves were
427 becoming a significant player of the emerging Arctic in autumn freezing. Climatology
428 suggested a big signal, but the detailed processes were not known. In 2015, the field cam-
429 paign documented the extent of sea state influences on the Arctic in autumn. The most
430 notable signal is the new prevalence of pancake ice near the ice edge, which is a direct
431 consequence of increasing wave activity. In this sense, the Arctic may be transitioning to a
432 state more similar to the Antarctic, where waves and pancake ice are ubiquitous.

433 Autumn refreezing in the western Arctic can now be summarized as a complex pro-
434 cess controlled by:

- 435 • ocean preconditioning by air-sea heat fluxes,
- 436 • wave-ice feedbacks (e.g., pancake formation, attenuation),
- 437 • ocean cooling during off-ice winds,
- 438 • ocean mixing during on-ice winds, and
- 439 • ice edge reversals during events.

440 These results and the products of this program are being used to improve forecast
441 and climate models. In addition to the challenge of two-way coupling in these models,
442 the event-driven nature of the key processes may be difficult for model tuning (though the
443 ample parameters measured or derived should allow model improvements through process
444 validation techniques). This new dataset is a leap forward in autumn Arctic observations,
445 in which one particularly large wave event was extensively measured. Of course, if events
446 drive the system, observations of numerous events will be required to make meaningful
447 progress in model development. Still, we expect this data set to be used extensively for
448 future studies, such as examining details of air-ice-ocean momentum transports and air-

449 ice-ocean interactions during off-ice wind events, which were more common than on-ice
450 events.

451 The papers contained within this special issue are the first round of analyses from
452 the field data and model developments. As always, there is more work to be done. The
453 data archive is available for continued analysis and model testing by an expanding set of
454 researchers. Although key processes have been identified and quantified, much remains to
455 be understood about the temporal and spatial scales over which these processes occur.

456 The complexity and variability of the upper ocean structure stands out within the
457 dataset as a remaining challenge. Significant efforts have been ongoing for decades to un-
458 derstand the inflow of Pacific Summer Water (PSW) over the Chukchi slope, the circu-
459 lation of the Beaufort Gyre, and the eddies that are generated near the boundaries. Even
460 with this context and climatology, however, it was not possible to make skillful predic-
461 tions of underway CTD observations during the Arctic Sea State campaign. The strength
462 of both the near surface temperature maximum (NSTM) and the PSW were highly vari-
463 able along the ship track. It is clear that the progression of the seasonal ice cover has a
464 strong influence on this upper ocean variability, but the atmospheric and advective sig-
465 nals driving the sea ice itself also show considerable variability. Therefore, to understand
466 the drivers of this tightly coupled air-sea-ice system, not only do the simultaneous air-sea-
467 ice interactions need to be considered, but also the far field and preconditioning factors
468 need to be addressed as well. A new program, the Stratified Ocean Dynamics in the Arc-
469 tic (www.apl.uw.edu/soda) aims to understand this variability with an observational cam-
470 paign over the 2018-2019 annual cycle.

471 The complexity of the sea ice remains another challenge. As demonstrated by the
472 extensive visual observations following the ASPECT protocols, sea ice is not easily char-
473 acterized by a few scalar parameters (though that is what coupled models would most eas-
474 ily use). This challenge is extreme during refreezing, when changing surface fluxes cause
475 rapid evolution of the new sea ice (e.g., Persson et al, this issue). Models such as CICE
476 and in situ observations must converge on a set of metrics that are most relevant to the
477 coupled dynamics and that capture the variability. Another new program, the Sea Ice Dy-
478 namics Experiment (SIDEX) will make progress on this topic with a 2020 campaign.

479 Finally, though the new wave-ice schemes in models like WAVEWATCH3 are im-
480 pressive in their ability to reproduce observations in a hindcast, there is still a fundamental
481 question as the mechanism(s) by which waves lose energy as they propagate through sea
482 ice. The new dataset is by far the most extensive observation of waves in sea ice collected
483 to date, yet the measurements are mostly the net effect of the wave-ice interactions, and
484 limited to the region less than 100 km from the open ocean. Direct measurements of col-
485 lisions, flexure, and turbulence within pancake ice are the next horizon for measurements
486 of wave-ice processes. To follow the evolution of these processes from the ice edge to
487 the interior pack ice requires larger spatial monitoring. More ambitious still, the message
488 from the Arctic Sea State program is clear: these specific interactions exist within a fully
489 coupled air-ocean-ice system, and such measurements would be incomplete without char-
490 acterizing the whole system simultaneously.

491 **Acknowledgments**

492 This program was supported by the Office of Naval Research, Code 32, under Program
493 Managers Drs. Scott Harper and Martin Jeffries. The crew of R/V Sikuliaq provide out-
494 standing support in collecting the field data, and the US National Ice Center, German
495 Aerospace Center (DLR), and European Space Agency facilitated the remote sensing col-
496 lections and daily analysis products. RADARSAT-2 Data and Products are from MacDon-
497 ald, Dettwiler, and Associates Ltd., courtesy of the U.S. National Ice Center

498 Data, supplemental material, and a cruise report can be found at
499 <http://www.apl.uw.edu/arcticseastate>

References

- 500
- 501 Arduin, F., and R. Magne (2007), Current effects on scattering of surface gravity waves
502 by bottom topography, *J. Fluid Mech.*, 576, 235–264.
- 503 Arduin, F., F. Collard, B. Chapron, F. Girard-Arduin, G. Guitton, A. Mouche, and J. E.
504 Stopa (2015), Estimates of ocean wave heights and attenuation in sea ice using the
505 sar wave mode on sentinel-1a, *Geophysical Research Letters*, 42(7), 2317–2325, doi:
506 10.1002/2014GL062940, 2014GL062940.
- 507 Arduin, F., P. Sutherland, M. Doble, and P. Wadhams (2016), Ocean waves across the
508 arctic: Attenuation due to dissipation dominates over scattering for periods longer
509 than 19 s, *Geophysical Research Letters*, pp. n/a–n/a, doi:10.1002/2016GL068204,
510 2016GL068204.
- 511 Arduin, F., J. Stopa, B. Chapron, F. Collard, M. Smith, J. Thomson, M. Doble,
512 B. Blomquist, O. Persson, C. O. C. III, and P. Wadhams (2017), Measuring ocean
513 waves in sea ice using SAR imagery: A quasi-deterministic approach evaluated with
514 Sentinel-1 and in situ data, *Remote Sensing of Environment*, 189, 211 – 222, doi:
515 <http://dx.doi.org/10.1016/j.rse.2016.11.024>.
- 516 Bennetts, L., A. Alberello, M. Meylan, C. Cavaliere, A. Babanin, and A. Toffoli (2015),
517 An idealised experimental model of ocean surface wave transmission by an ice floe,
518 *Ocean Modelling*, 96(Part 1), 85 – 92, doi:<https://doi.org/10.1016/j.ocemod.2015.03.001>,
519 waves and coastal, regional and global processes.
- 520 Cheng, S., W. E. Rogers, J. Thomson, M. Smith, M. J. Doble, P. Wadhams, A. L. Ko-
521 hout, B. Lund, O. P. Persson, C. O. Collins, S. F. Ackley, F. Montiel, and H. H. Shen
522 (2017), Calibrating a viscoelastic sea ice model for wave propagation in the arctic
523 fall marginal ice zone, *Journal of Geophysical Research: Oceans*, 122, n/a–n/a, doi:
524 10.1002/2017JC013275.
- 525 Collins, C., and W. Rogers (2017), A source term for wave attenuation by sea ice in
526 WAVEWATCH III: IC4, *Tech. Rep. NRL/MR/7320-17-9726*, Naval Research Laboratory.
- 527 Collins, C. O., W. E. Rogers, A. Marchenko, and A. V. Babanin (2015), In situ measure-
528 ments of an energetic wave event in the arctic marginal ice zone, *Geophysical Research*
529 *Letters*, pp. n/a–n/a, doi:10.1002/2015GL063063.
- 530 Collins, C. O., W. E. Rogers, and B. Lund (2017a), An investigation into the dispersion of
531 ocean surface waves in sea ice, *Ocean Dynamics*, 67(2), 263–280, doi:10.1007/s10236-
532 016-1021-4.
- 533 Collins, C. O., B. Blomquist, O. Persson, B. Lund, W. E. Rogers, J. Thomson, D. Wang,
534 M. Smith, M. Doble, P. Wadhams, A. Kohout, C. Fairall, and H. C. Graber (2017b),
535 Doppler correction of wave frequency spectra measured by underway vessels, *Journal*
536 *of Atmospheric and Oceanic Technology*, 34(2), 429–436, doi:10.1175/JTECH-D-16-
537 0138.1.
- 538 Doble, M. J., and J.-R. Bidlot (2013), Wave buoy measurements at the antarctic
539 sea ice edge compared with an enhanced ecmwf wam: Progress towards global
540 waves-in-ice modelling, *Ocean Modelling*, 70(Supplement C), 166 – 173, doi:
541 <https://doi.org/10.1016/j.ocemod.2013.05.012>, ocean Surface Waves.
- 542 Fox, C., and V. A. Squire (1994), On the Oblique Reflexion and Transmission of Ocean
543 Waves at Shore Fast Sea Ice, *Philosophical Transactions of the Royal Society of London*
544 *Series A*, 347, 185–218, doi:10.1098/rsta.1994.0044.
- 545 Francis, O. P., G. G. Panteleev, and D. E. Atkinson (2011), Ocean wave conditions in the
546 Chukchi Sea from satellite and in situ observations, *Geophys. Res. Lett.*, 38(L24610),
547 doi:10.1029/2011GL049839.
- 548 Gebhardt, C., J.-R. Bidlot, J. Gemmrich, S. Lehner, A. Pleskachevsky, and W. Rosenthal
549 (2016), Wave observation in the marginal ice zone with the terrasar-x satellite, *Ocean*
550 *Dynamics*, 66(6), 839–852, doi:10.1007/s10236-016-0957-8.
- 551 Gebhardt, C., J. R. Bidlot, S. Jacobsen, S. Lehner, P. O. G. Persson, and A. L.
552 Pleskachevsky (2017), The potential of terrasar-x to observe wind wave interaction at
553 the ice edge, *IEEE Journal of Selected Topics in Applied Earth Observations and Remote*

554 *Sensing*, 10(6), 2799–2809, doi:10.1109/JSTARS.2017.2652124.

555 Gemrich, J., J. Thomson, W. E. Rogers, A. Pleskachevsky, and S. Lehner (2016), Spa-
556 tial characteristics of ocean surface waves, *Ocean Dynamics*, 66(8), 1025–1035, doi:
557 10.1007/s10236-016-0967-6.

558 Inoue, J., M. E. Hori, Y. Tachibana, and T. Kikuchi (2010), A polar low embedded in a
559 blocking high over the pacific arctic, *Geophysical Research Letters*, 37(14), n/a–n/a, doi:
560 10.1029/2010GL043946, 114808.

561 Jackson, J. M., E. C. Carmack, F. A. McLaughlin, S. E. Allen, and R. G. Ingram (2010),
562 Identification, characterization, and change of the near-surface temperature maximum
563 in the canada basin, 1993–2008, *Journal of Geophysical Research: Oceans*, 115(C5),
564 n/a–n/a, doi:10.1029/2009JC005265, c05021.

565 Jeffries, M. O., J. E. Overland, and D. K. Perovich (2013), The Arctic shifts to a new nor-
566 mal, *Physics Today*, 66(10), doi:10.1063/PT.3.2147.

567 Khon, V. C., I. I. Mokhov, F. A. Pogarskiy, A. Babanin, K. Dethloff, A. Rinke, and
568 H. Matthes (2014), Wave heights in the 21st century arctic ocean simulated with
569 a regional climate model, *Geophysical Research Letters*, 41(8), 2956–2961, doi:
570 10.1002/2014GL059847, 2014GL059847.

571 Kohout, A. L., M. J. M. Williams, S. M. Dean, and M. H. Meylan (2014), Storm-induced
572 sea-ice breakup and the implications for ice extent, *Nature*, 509, 604 EP –.

573 Lee, C., and J. Thomson (2017), An autonomous approach to observing the seasonal ice
574 zone, *Oceanography Magazine*, 30.

575 Li, J., S. Mondal, and H. H. Shen (2015a), Sensitivity analysis of a viscoelastic param-
576 eterization for gravity wave dispersion in ice covered seas, *Cold Regions Science and*
577 *Technology*, 120, 63 – 75, doi:https://doi.org/10.1016/j.coldregions.2015.09.009.

578 Li, J., A. L. Kohout, and H. H. Shen (2015b), Comparison of wave propagation through
579 ice covers in calm and storm conditions, *Geophysical Research Letters*, 42(14), 5935–
580 5941, doi:10.1002/2015GL064715, 2015GL064715.

581 Li, J., A. L. Kohout, M. J. Doble, P. Wadhams, C. Guan, and H. H. Shen (2017), Rollover
582 of apparent wave attenuation in ice covered seas, *Journal of Geophysical Research:*
583 *Oceans*, pp. n/a–n/a, doi:10.1002/2017JC012978.

584 Li, J.-G. (2016), Ocean surface waves in an ice-free arctic ocean, *Ocean Dynamics*, 66(8),
585 989–1004, doi:10.1007/s10236-016-0964-9.

586 Liu, Q., A. V. Babanin, S. Zieger, I. R. Young, and C. Guan (2016), Wind and wave cli-
587 mate in the arctic ocean as observed by altimeters, *Journal of Climate*, 29(22), 7957–
588 7975, doi:10.1175/JCLI-D-16-0219.1.

589 Long, Z., and W. Perrie (2013), Impacts of climate change on fresh water content
590 and sea surface height in the Beaufort Sea, *Ocean Modelling*, 71, 127–139, doi:
591 http://dx.doi.org/10.1016/j.ocemod.2013.05.006.

592 Long, Z., and W. Perrie (2015), Scenario changes of Atlantic water in the Arctic Ocean, *J.*
593 *Climate*, 28, 552305,548, doi:http://dx.doi.org/10.1175/JCLI-D-14-00522.1.

594 Long, Z., and W. Perrie (2017), Changes in ocean temperature in the Barents sea in the
595 twenty-first century, *Journal of Climate*, 30(15), 5901–5921, doi:10.1175/JCLI-D-16-
596 0415.1.

597 Lund, B., H. C. Graber, K. Hessner, and N. J. Williams (2015), On shipboard marine x-
598 band radar near-surface current “calibration”, *Journal of Atmospheric and Oceanic Tech-*
599 *nology*, 32(10), 1928–1944, doi:10.1175/JTECH-D-14-00175.1.

600 Lund, B., C. J. Zappa, H. C. Graber, and A. Cifuentes-Lorenzen (2017), Shipboard wave
601 measurements in the southern ocean, *Journal of Atmospheric and Oceanic Technology*,
602 34(9), 2113–2126, doi:10.1175/JTECH-D-16-0212.1.

603 Martin, T., M. Tsamados, D. Schroeder, and D. L. Feltham (2016), The impact of variable
604 sea ice roughness on changes in arctic ocean surface stress: A model study, *Journal of*
605 *Geophysical Research: Oceans*, pp. n/a–n/a, doi:10.1002/2015JC011186.

606 Maslanik, J. A., C. Fowler, J. C. Stroeve, S. Drobot, J. Zwally, D. Yi, and W. Emery
607 (2007), A younger, thinner Arctic ice cover: Increased potential for rapid, extensive sea-

ice loss, *Geophys. Res. Lett.*, 34(34).

Montiel, F., and V. A. Squire (2017), Modelling wave-induced sea ice break-up in the marginal ice zone, *Proceedings of the Royal Society of London A: Mathematical, Physical and Engineering Sciences*, 473(2206), doi:10.1098/rspa.2017.0258.

Montiel, F., V. A. Squire, and L. G. Bennetts (2016), Attenuation and directional spreading of ocean wave spectra in the marginal ice zone, *J. Fluid Mech.*, 790, 492–522.

Mosig, J. E. M., F. Montiel, and V. A. Squire (2015), Comparison of viscoelastic-type models for ocean wave attenuation in ice-covered seas, *Journal of Geophysical Research: Oceans*, 120(9), 6072–6090, doi:10.1002/2015JC010881.

Perovich, D. K., B. Light, H. Eicken, K. F. Jones, K. Runciman, and S. V. Nghiem (2007), Increasing solar heating of the arctic ocean and adjacent seas, 1979–2005: Attribution and role in the ice-albedo feedback, *Geophysical Research Letters*, 34(19), n/a–n/a, doi: 10.1029/2007GL031480, 119505.

Pingree-Shippee, K. A., N. J. Shippee, and D. E. Atkinson (2016), Overview of Bering and Chukchi sea wave states for four severe storms following common synoptic tracks, *Journal of Atmospheric and Oceanic Technology*, 33(2), 283–302, doi:10.1175/JTECH-D-15-0153.1.

Rogers, W., and M. D. Orzech (2013), Implementation and testing of ice and mud source functions in WAVEWATCH III, *Memorandum Report NRL/MR/7320–13-9462*, Naval Research Laboratory.

Rogers, W. E., J. Thomson, H. H. Shen, M. J. Doble, P. Wadhams, and S. Cheng (2016), Dissipation of wind waves by pancake and frazil ice in the autumn beaufort sea, *Journal of Geophysical Research: Oceans*, 121(11), 7991–8007, doi:10.1002/2016JC012251.

Serreze, M. C., A. D. Crawford, J. C. Stroeve, A. P. Barrett, and R. A. Woodgate (2016), Variability, trends, and predictability of seasonal sea ice retreat and advance in the chukchi sea, *Journal of Geophysical Research: Oceans*, pp. n/a–n/a, doi: 10.1002/2016JC011977.

Smith, M., and J. Thomson (2016), Scaling observations of surface waves in the beaufort sea, *Elem Sci Anth*, 4(000097), doi:10.12952/journal.elementa.000097.

Squire, V. A. (2007), Of ocean waves and sea ice revisited, *Cold Regions Sci. Tech.*, 49, 110–133.

Squire, V. A., J. P. Dugan, P. Wadhams, P. J. Rottier, and A. K. Liu (1995), Of ocean waves and sea ice, *Annu. Rev. Fluid Mech.*, 27, 115–168.

Stammerjohn, S., R. Massom, D. Rind, and D. Martinson (2012), Regions of rapid sea ice change: An inter-hemispheric seasonal comparison, *Geophysical Research Letters*, 39(6), n/a–n/a, doi:10.1029/2012GL050874, 106501.

Steele, M., and W. Ermold (2015), Loitering of the retreating sea ice edge in the arctic seas, *Journal of Geophysical Research: Oceans*, 120(12), 7699–7721, doi: 10.1002/2015JC011182.

Stopa, J. E., F. Ardhuin, and F. Girard-Ardhuin (2016), Wave-climate in the Arctic 1992–2014: seasonality, trends, and wave-ice influence, *The Cryosphere*, 10(4), 1605–1629, doi:10.5194/tc-10-1605-2016.

Stroeve, J. C., A. D. Crawford, and S. Stammerjohn (2016), Using timing of ice retreat to predict timing of fall freeze-up in the arctic, *Geophysical Research Letters*, 43(12), 6332–6340, doi:10.1002/2016GL069314, 2016GL069314.

Sutherland, P., and J.-C. Gascard (2016), Airborne remote sensing of ocean wave directional wavenumber spectra in the marginal ice zone, *Geophysical Research Letters*, pp. n/a–n/a, doi:10.1002/2016GL067713, 2016GL067713.

The WAVEWATCH III[®] Development Group (2016), User manual and system documentation of WAVEWATCH III version 5.16, *Tech. Rep. 329*, NOAA/NWS/NCEP/Marine Modeling and Analysis Branch.

Thomson, J., and W. E. Rogers (2014), Swell and sea in the emerging Arctic Ocean, *Geophysical Research Letters*, pp. n/a–n/a, doi:10.1002/2014GL059983.

- 661 Thomson, J., V. Squire, S. Ackley, E. Rogers, A. Babanin, P. Guest, T. Maksym, P. Wad-
662 hams, S. Stammerjohn, C. Fairall, O. Persson, M. Doble, H. Graber, H. Shen, J. Gemm-
663 rich, S. Lehner, B. Holt, T. Williams, M. Meylan, and J. Bidlot (2013), Science plan:
664 Sea state and boundary layer physics of the emerging Arctic Ocean, *Technical Report*
665 *1306*, Applied Physics Laboratory, University of Washington.
- 666 Thomson, J., Y. Fan, S. Stammerjohn, J. Stopa, W. E. Rogers, F. Girard-Ardhuin,
667 F. Ardhuin, H. Shen, W. Perrie, H. Shen, S. Ackley, A. Babanin, Q. Liu, P. Guest,
668 T. Maksym, P. Wadhams, C. Fairall, O. Persson, M. Doble, H. Graber, B. Lund,
669 V. Squire, J. Gemmrich, S. Lehner, B. Holt, M. Meylan, J. Brozena, and J.-R. Bidlot
670 (2016), Emerging trends in the sea state of the beaufort and chukchi seas, *Ocean Mod-*
671 *elling*, *105*, 1 – 12, doi:<http://dx.doi.org/10.1016/j.ocemod.2016.02.009>.
- 672 Thomson, J., S. Ackley, H. H. Shen, and W. E. Rogers (2017), The balance of ice, waves,
673 and winds in the arctic autumn, *Eos*, *98*, doi:<https://doi.org/10.1029/2017EO066029>.
- 674 Tolman, H. L. (2003), Treatment of unresolved islands and ice in wind wave models,
675 *Ocean Modeling*, *5*, 219–231.
- 676 Tolman, H. L., and D. Chalikov (1996), Source terms in a third-generation wind wave
677 model, *Journal of Physical Oceanography*, *26*(11), 2497–2518, doi:10.1175/1520-
678 0485(1996)026<2497:STIATG>2.0.CO;2.
- 679 Wadhams, P., V. A. Squire, D. J. Goodman, A. M. Cowan, and S. C. Moore (1988), The
680 attenuation rates of ocean waves in the marginal ice zone, *J. Geophys. Res.*, *93*(C6),
681 6799–6818.
- 682 Wang, D., and R. Allard (2012), Validation of the operational performance of NAVO
683 SHARC METOC and wave sensor systems, *Tech. rep.*, Naval Research Laboratory.
- 684 Wang, J., H.-M. Kim, and E. K. M. Chang (2017), Changes in northern hemisphere winter
685 storm tracks under the background of arctic amplification, *Journal of Climate*, *30*(10),
686 3705–3724, doi:10.1175/JCLI-D-16-0650.1.
- 687 Wang, R., and H. H. Shen (2010), Gravity waves propagating into an ice-covered ocean:
688 A viscoelastic model, *Journal of Geophysical Research: Oceans*, *115*(C6), n/a–n/a, doi:
689 10.1029/2009JC005591, c06024.
- 690 Wang, X. L., Y. Feng, V. R. Swail, and A. Cox (2015), Historical changes in the Beaufort-
691 Chukchi-Bering seas surface winds and waves, 1971-2013, *Journal of Climate*, doi:
692 10.1175/JCLI-D-15-0190.1.
- 693 Zhao, X., and H. Shen (2016), A diffusion approximation for ocean wave scat-
694 terings by randomly distributed ice floes, *Ocean Modelling*, *107*, 21 – 27, doi:
695 <https://doi.org/10.1016/j.ocemod.2016.09.014>.
- 696 Zippel, S., and J. Thomson (2016), Air-sea interactions in the marginal ice zone, *Elem Sci*
697 *Anth*, *4*(000095).

Figure 1.

Author Manuscript

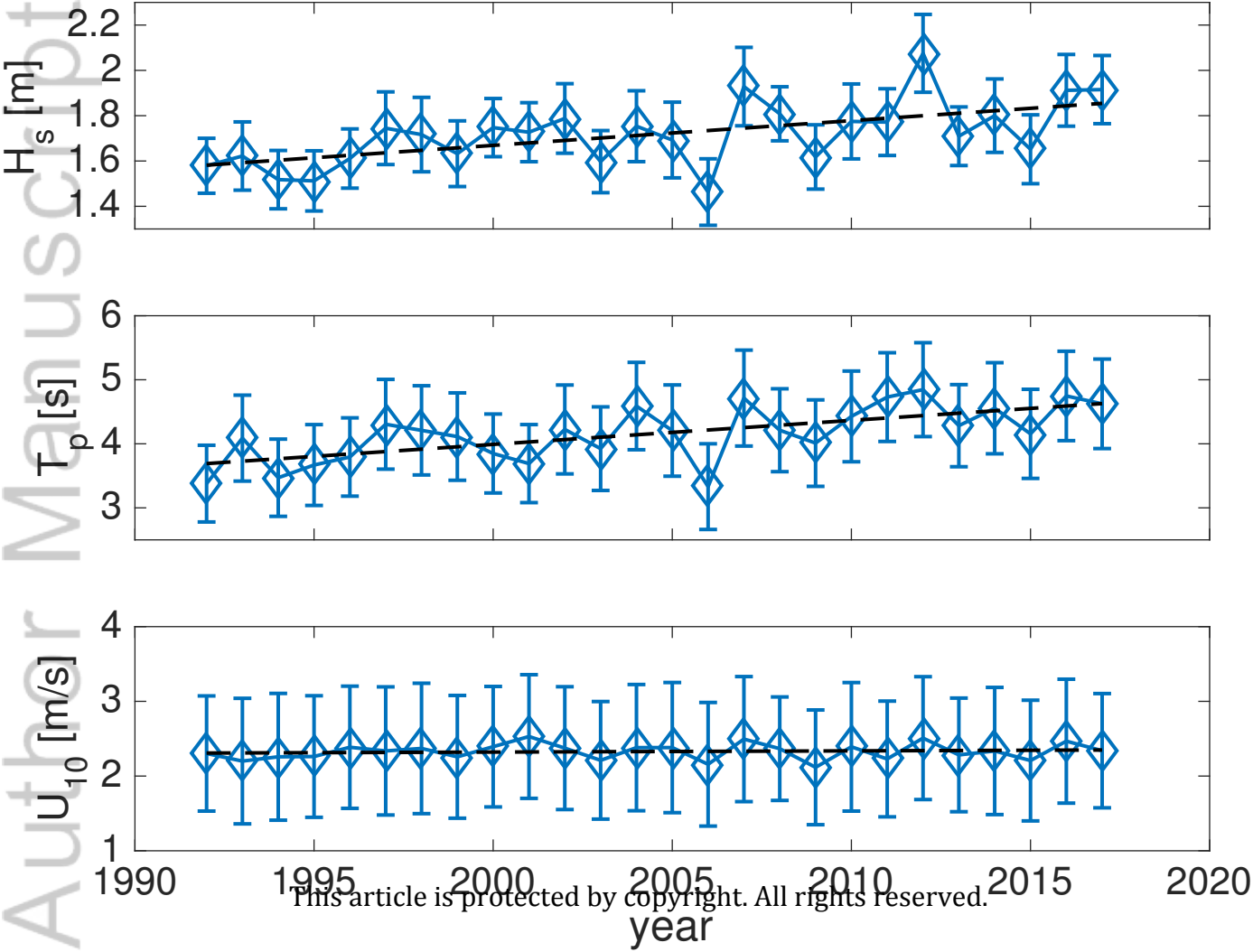


Figure 2.

Author Manuscript

10-Nov-2015 00:00:00 UTC
WW3 sig. wave height (m) and mean wv. dir.

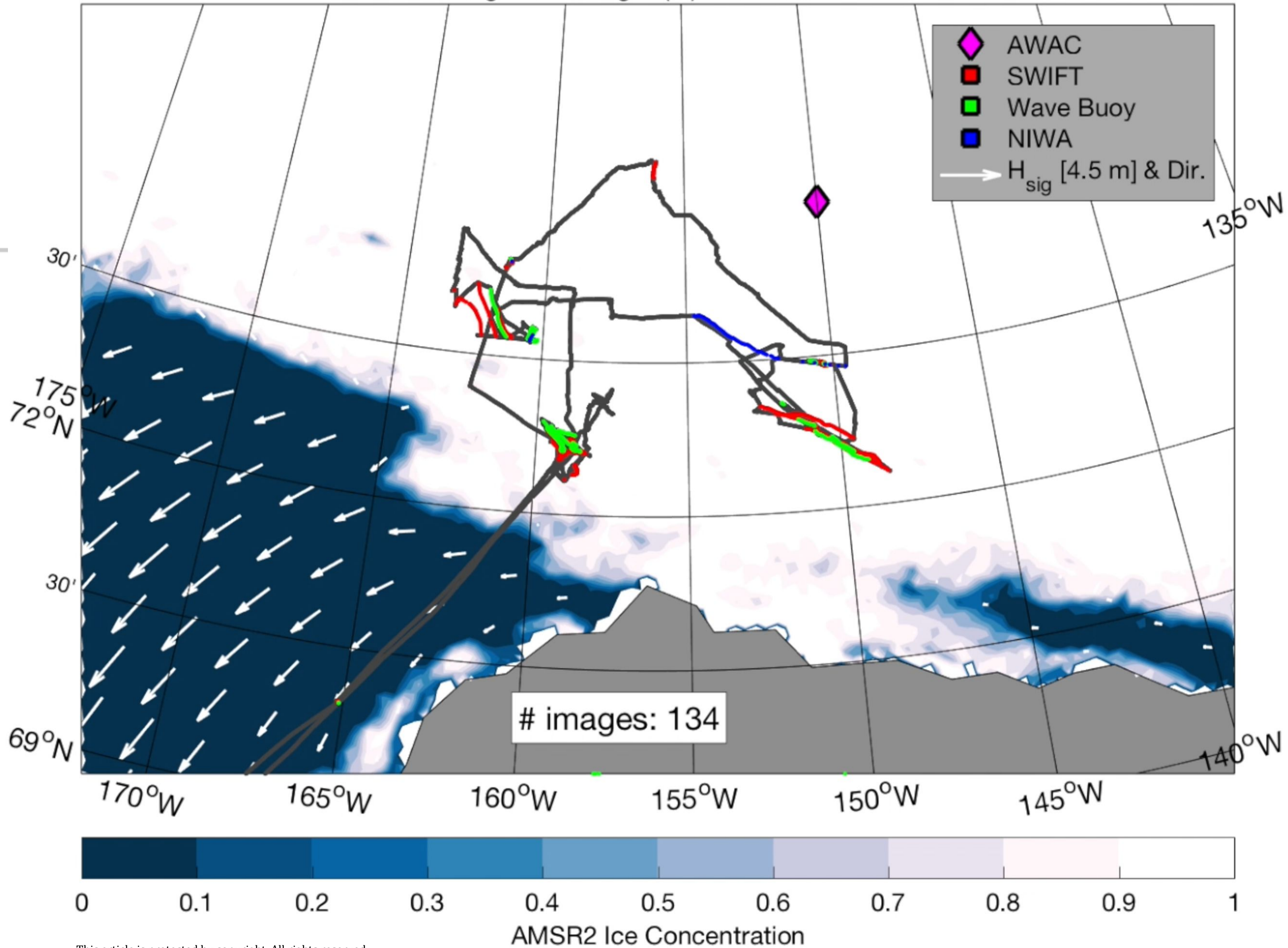
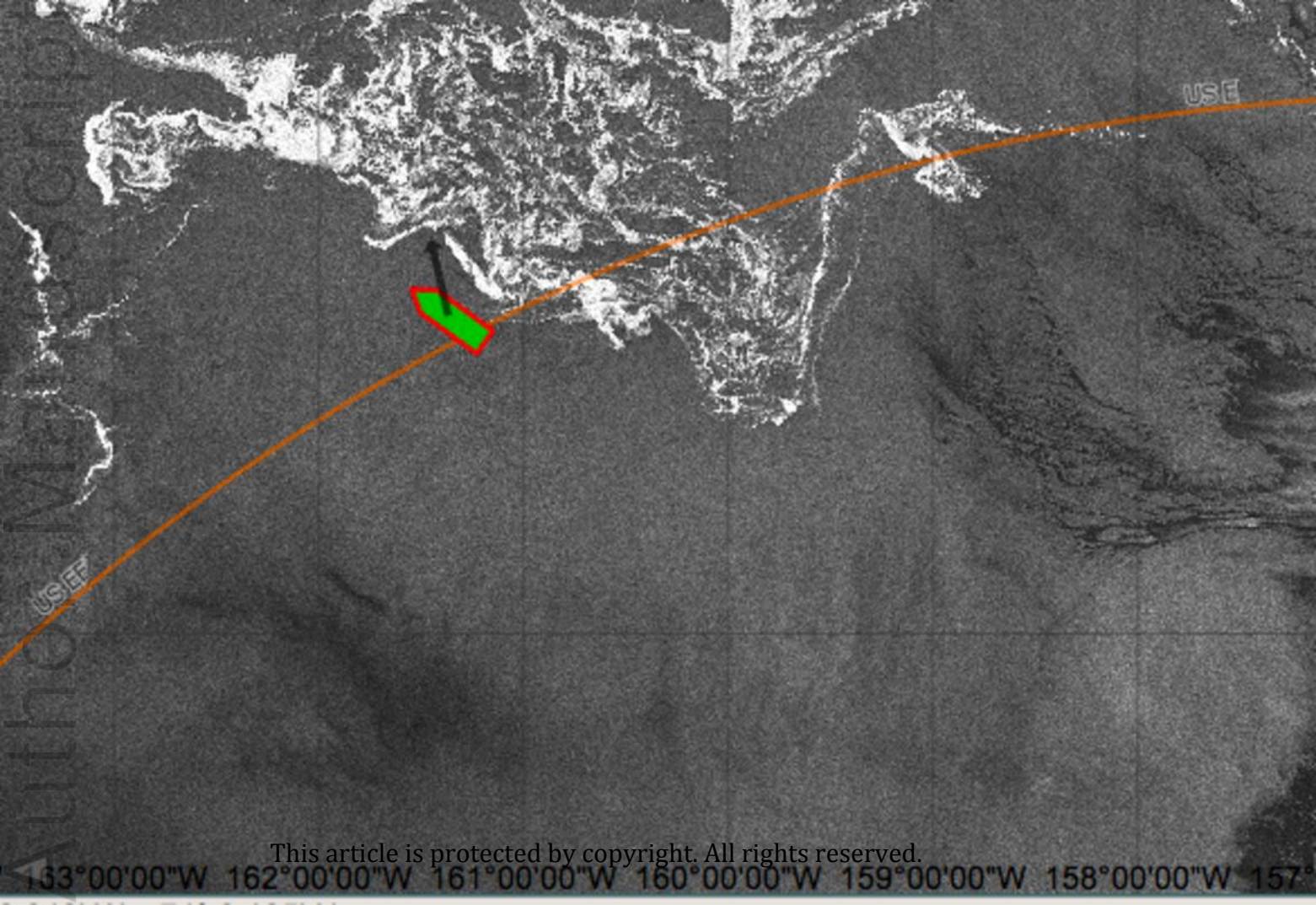


Figure 3.

Author Manuscript



This article is protected by copyright. All rights reserved.

163°00'00"W 162°00'00"W 161°00'00"W 160°00'00"W 159°00'00"W 158°00'00"W 157°

Figure 4.

Author Manuscript

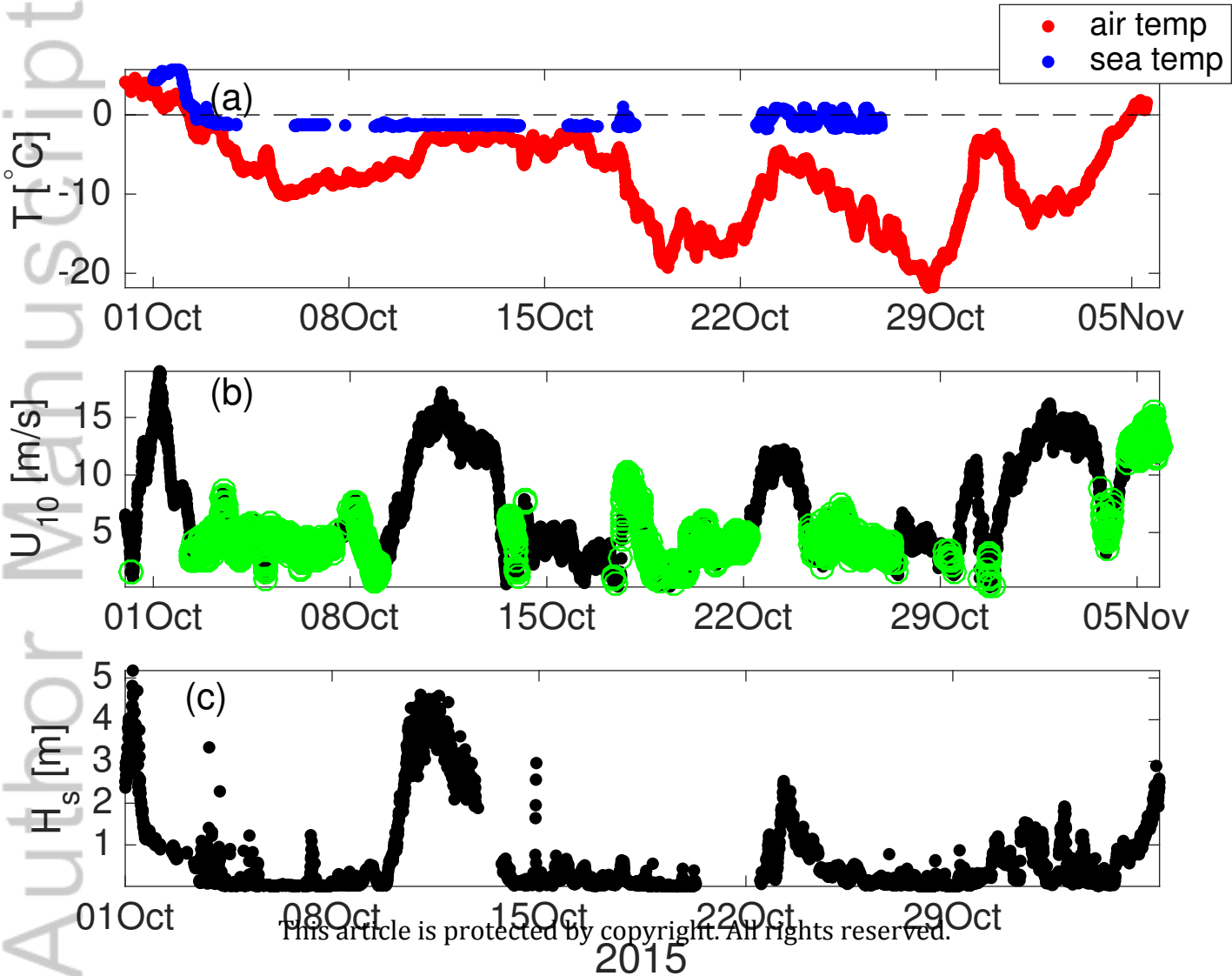


Figure 5.

Author Manuscript

Oct 10 2326 UTC

8.2 m/s /96°

$T_{a15} = -6.5^{\circ} \text{C}$

$T_s = -1.3^{\circ} \text{C}$

$SW_n = 29 \text{ W m}^{-2}$

$LW_n = -31 \text{ W m}^{-2}$

$H_{sb} = -65 \text{ W m}^{-2}$

$H_{lo} = -49 \text{ W m}^{-2}$

$F_{atm} = -115 \text{ W m}^{-2}$

Oct 12 2228 UTC

14.0 m/s /114°

$T_{a15} = -2.8^{\circ} \text{C}$

$T_s = -1.3^{\circ} \text{C}$

$SW_n = 24 \text{ W m}^{-2}$

$LW_n = -13 \text{ W m}^{-2}$

$H_{sb} = -26 \text{ W m}^{-2}$

$H_{lo} = -44 \text{ W m}^{-2}$

$F_{atm} = -59 \text{ W m}^{-2}$

This article is protected

Figure 6.

Author Manuscript

PDFs October: SeaState (2015) vs WW3 hindcast

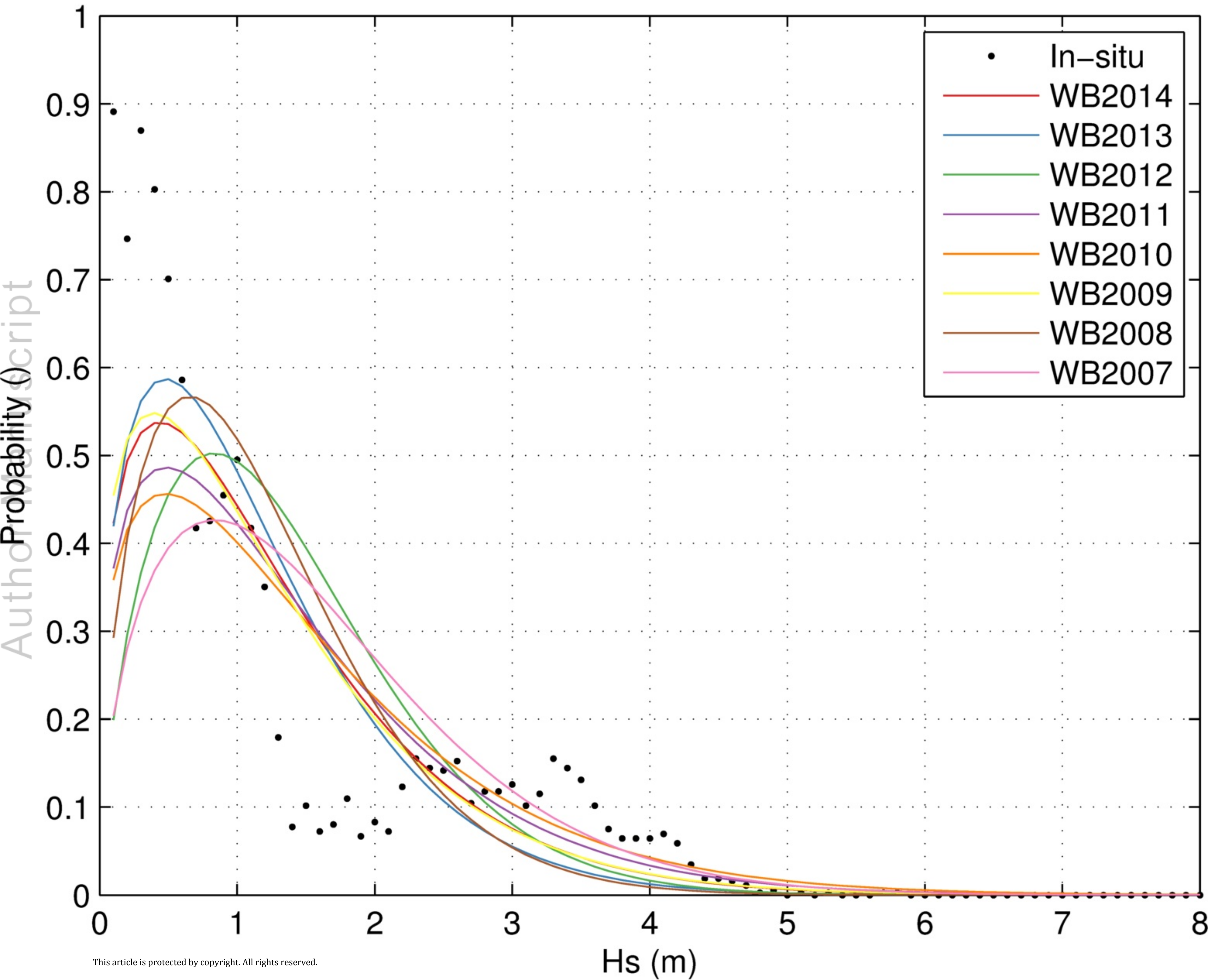


Figure 7.

Author Manuscript

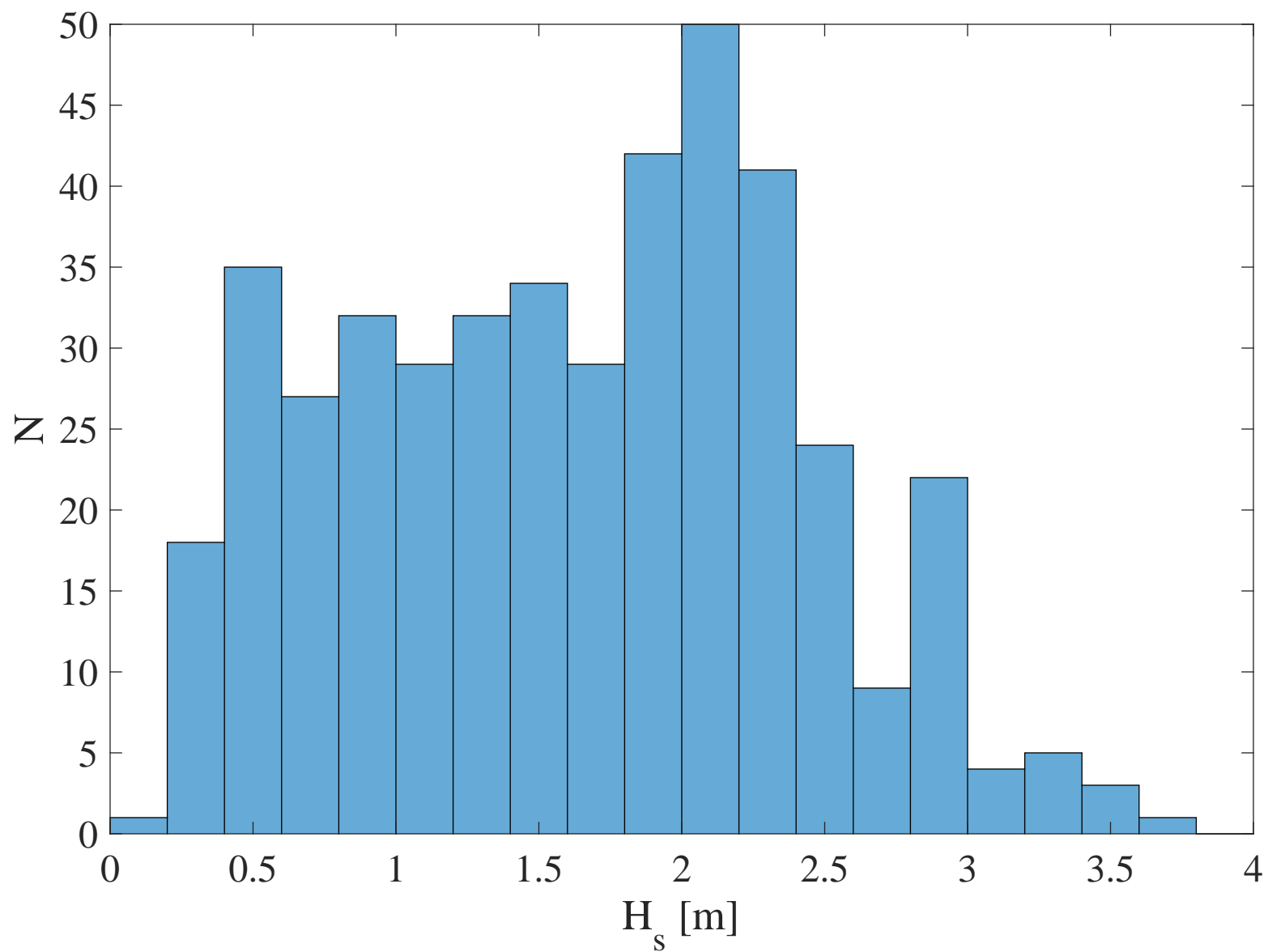


Figure 8.

Author Manuscript

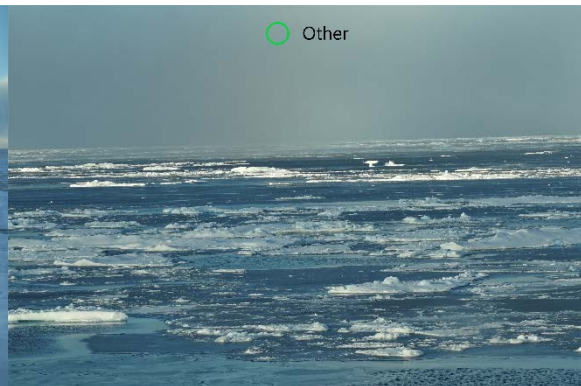
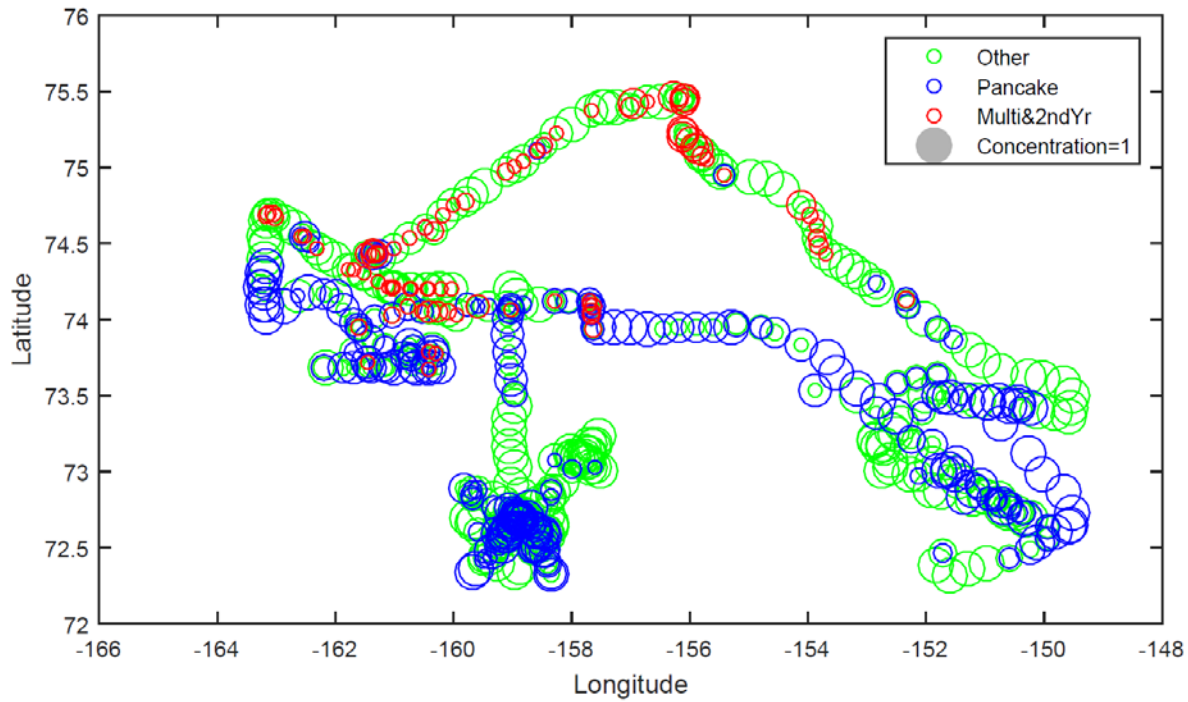


Figure 9.

Author Manuscript

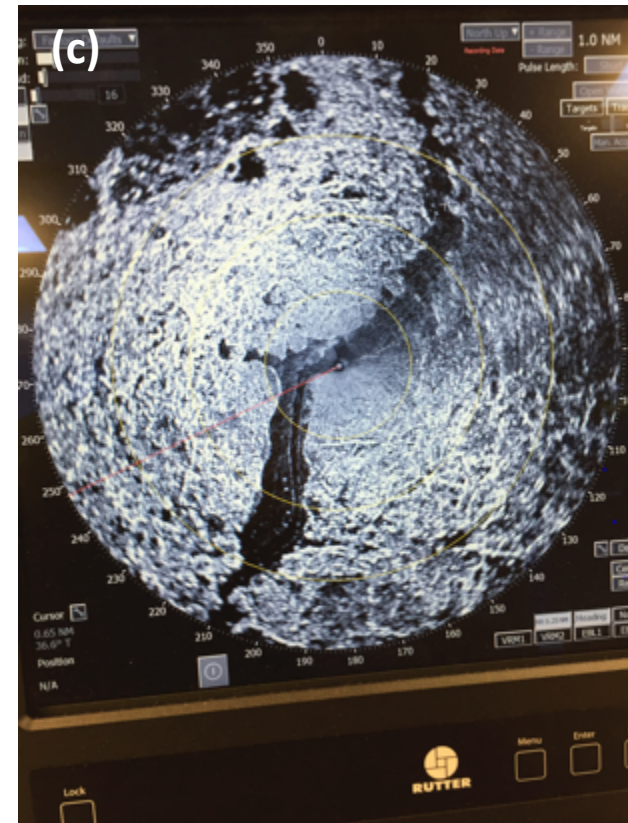
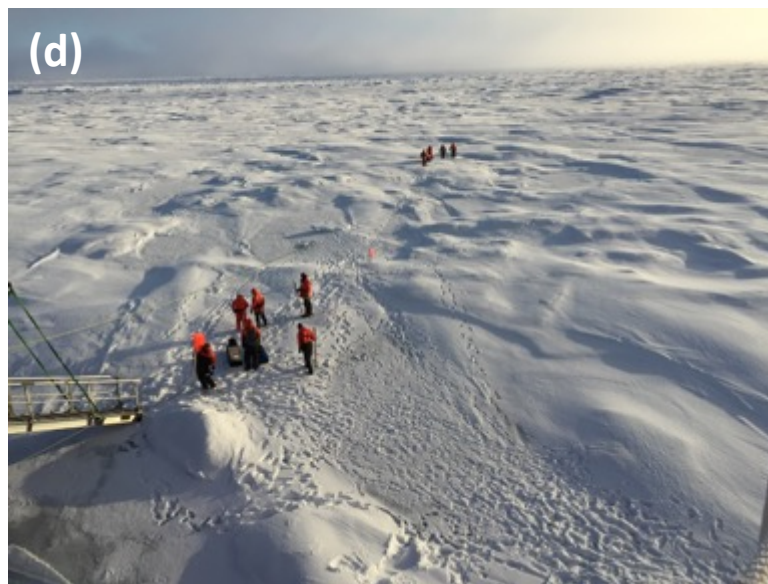
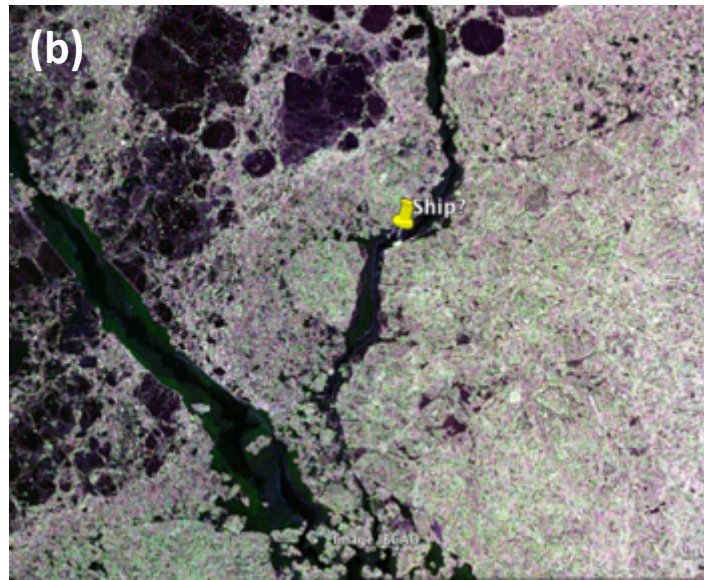
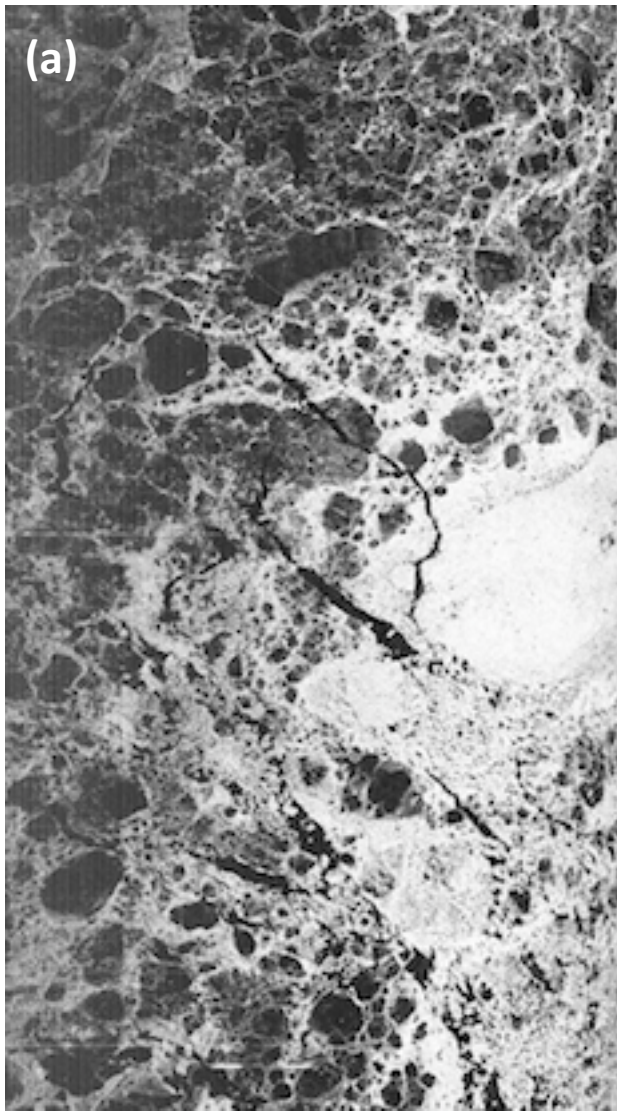
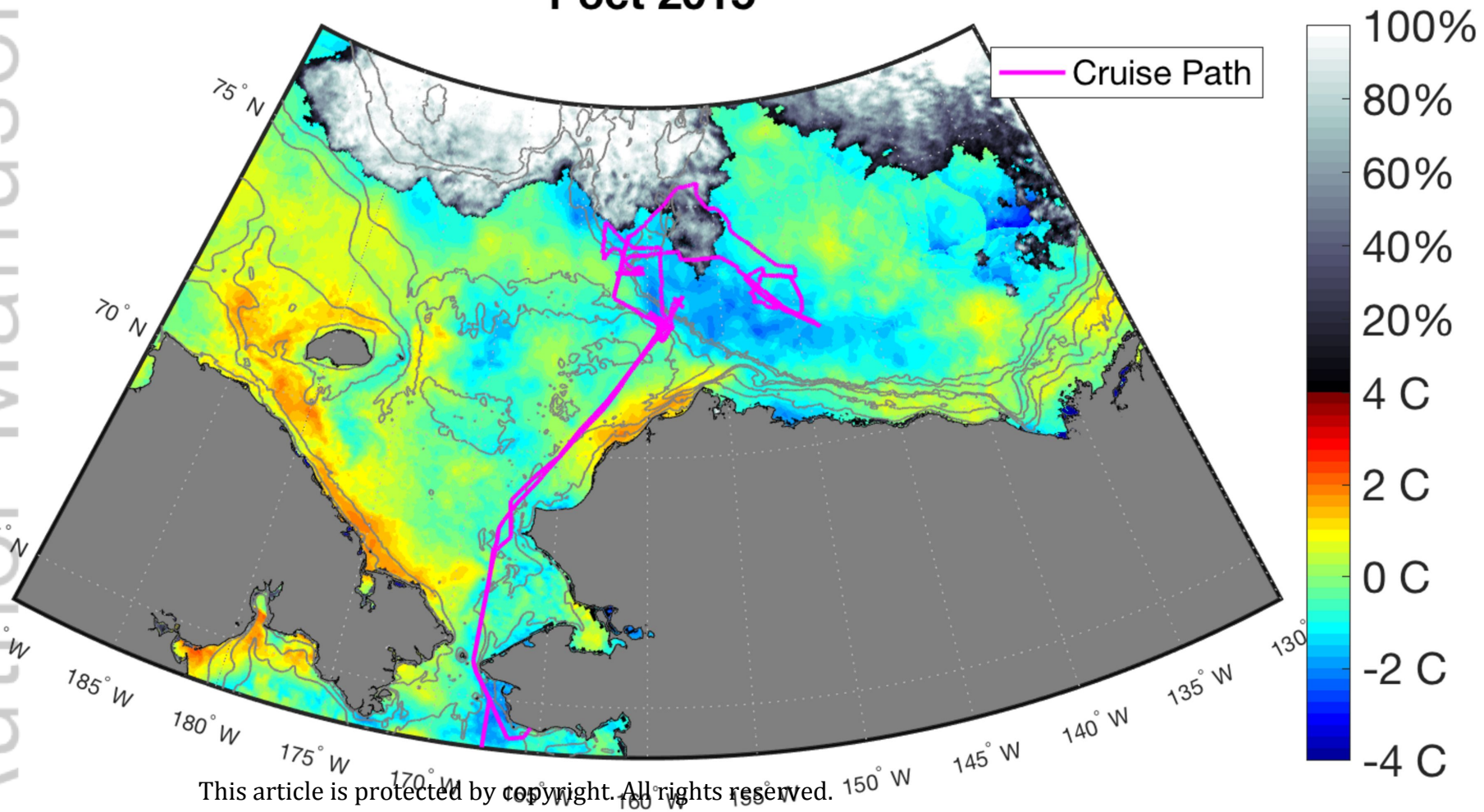


Figure 10.

Author Manuscript

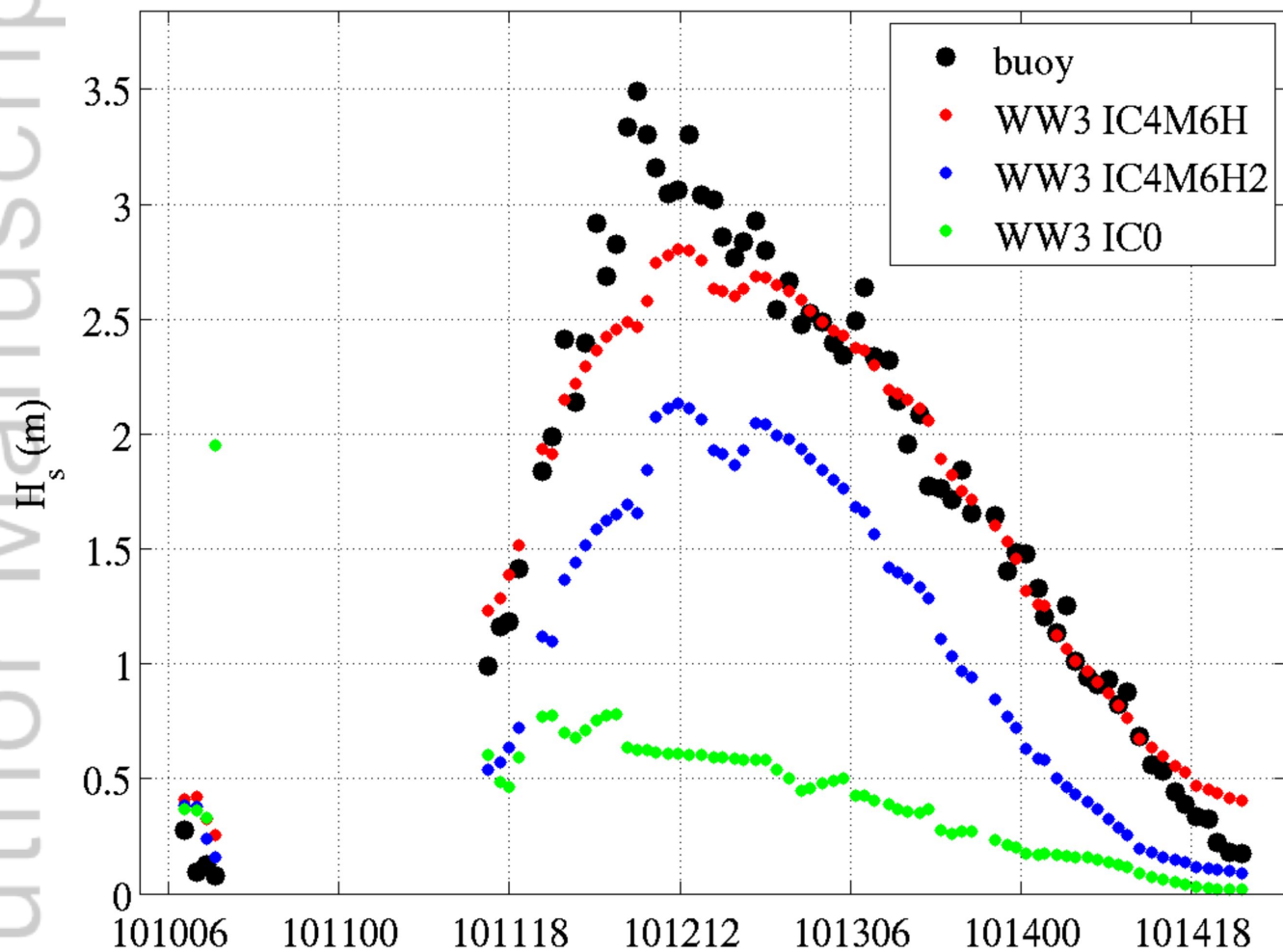
Sea ice concentration and sea surface temperature anomaly 1 oct 2015



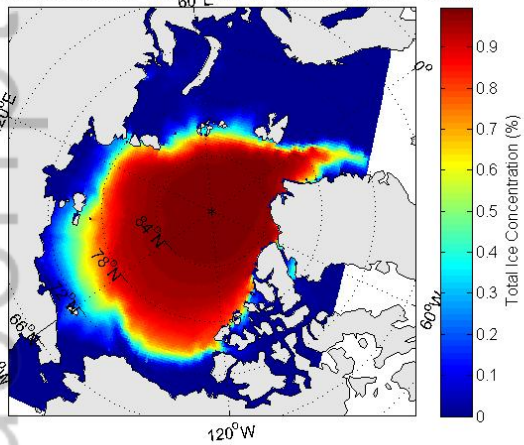
This article is protected by copyright. All rights reserved.

Figure 11.

Author Manuscript

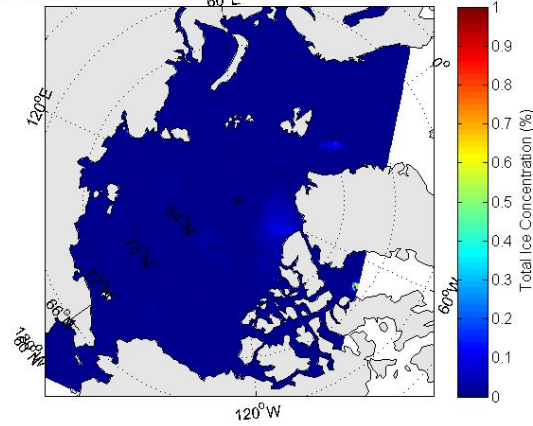


30 years mean ice coverage (Present 1970 - 1999)



120°W

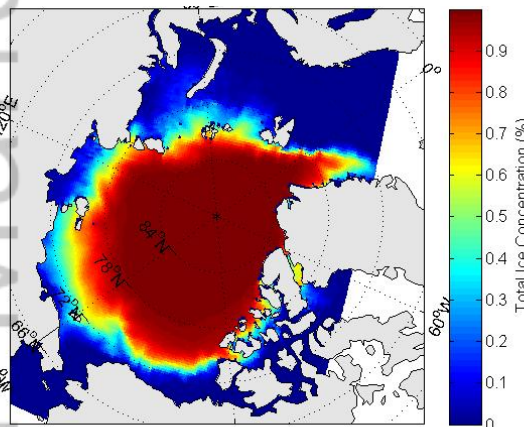
30 years mean ice coverage (Future 2070 - 2099)



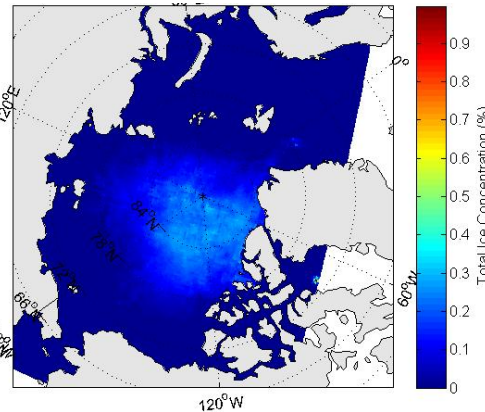
120°W

CIOM: A1B scenario

August

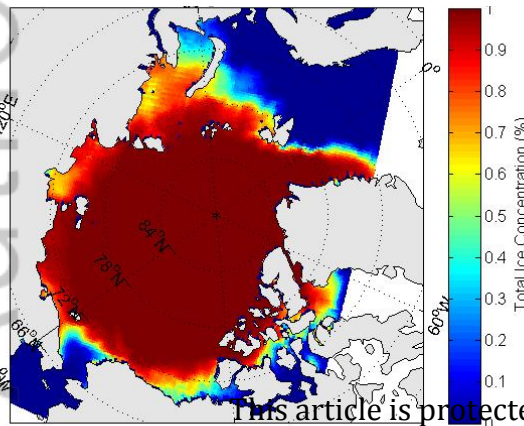


120°W

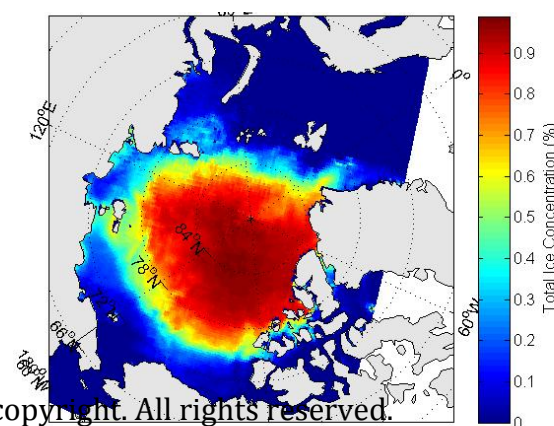


120°W

September

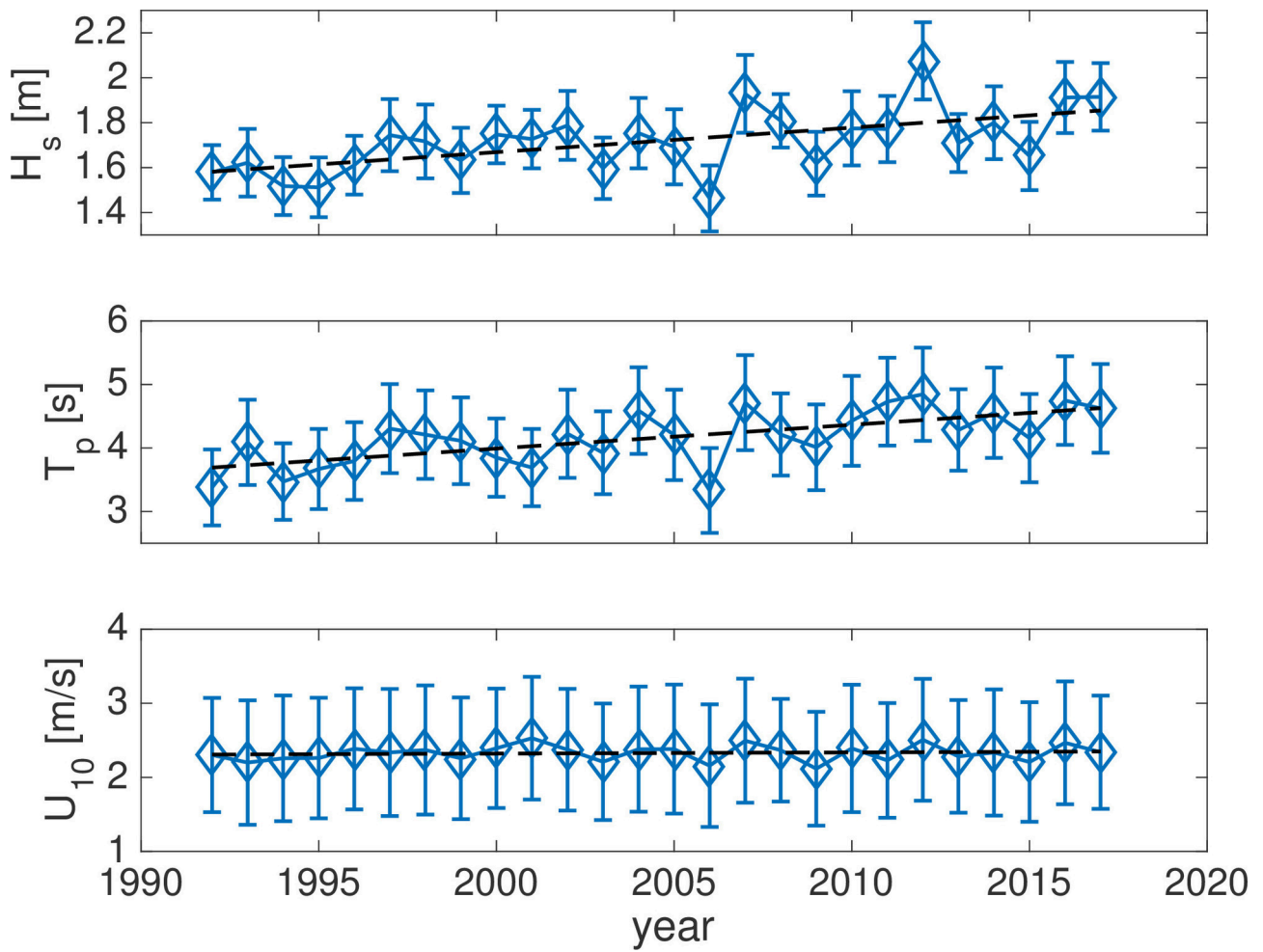


120°W



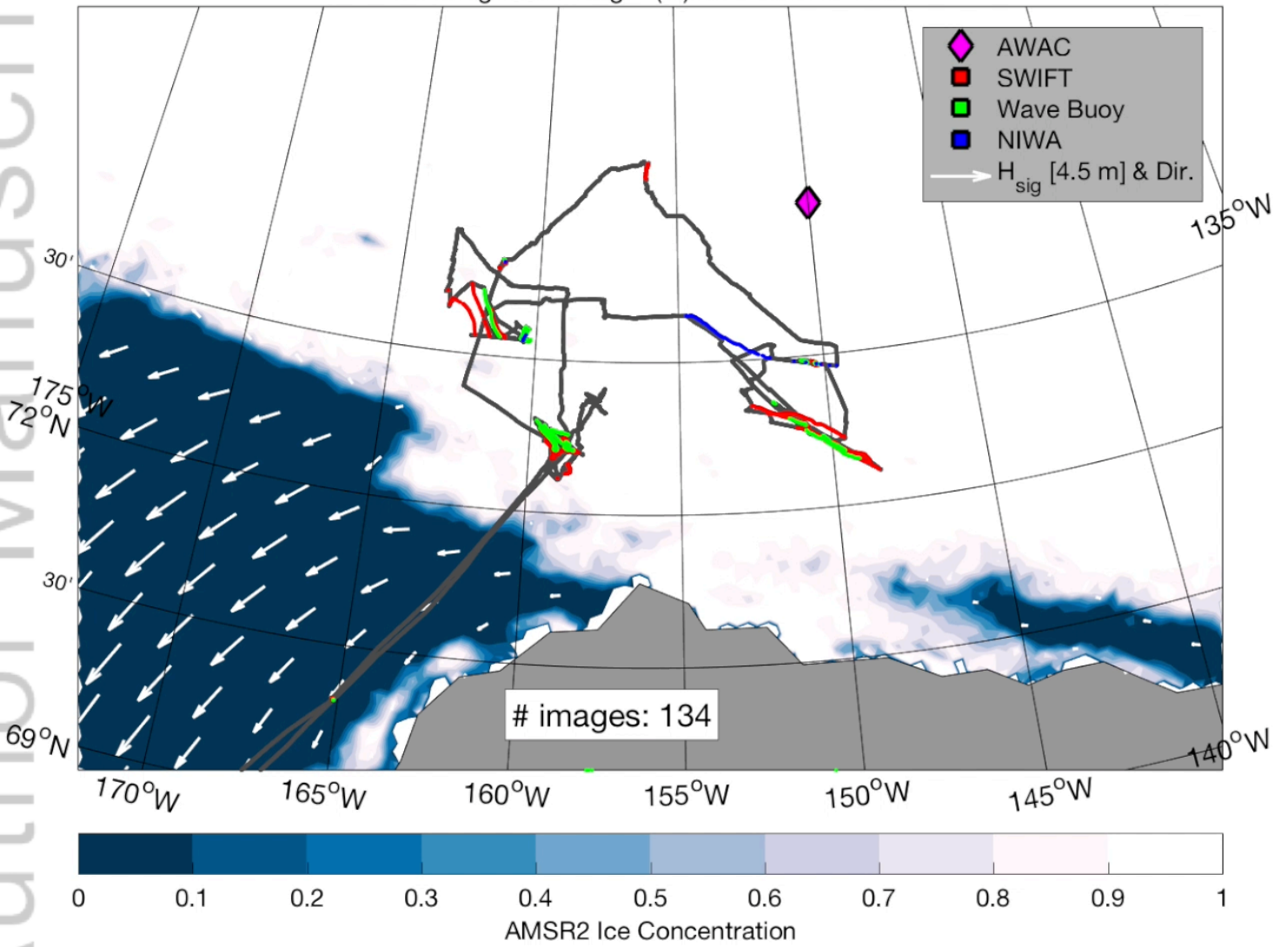
120°W

October

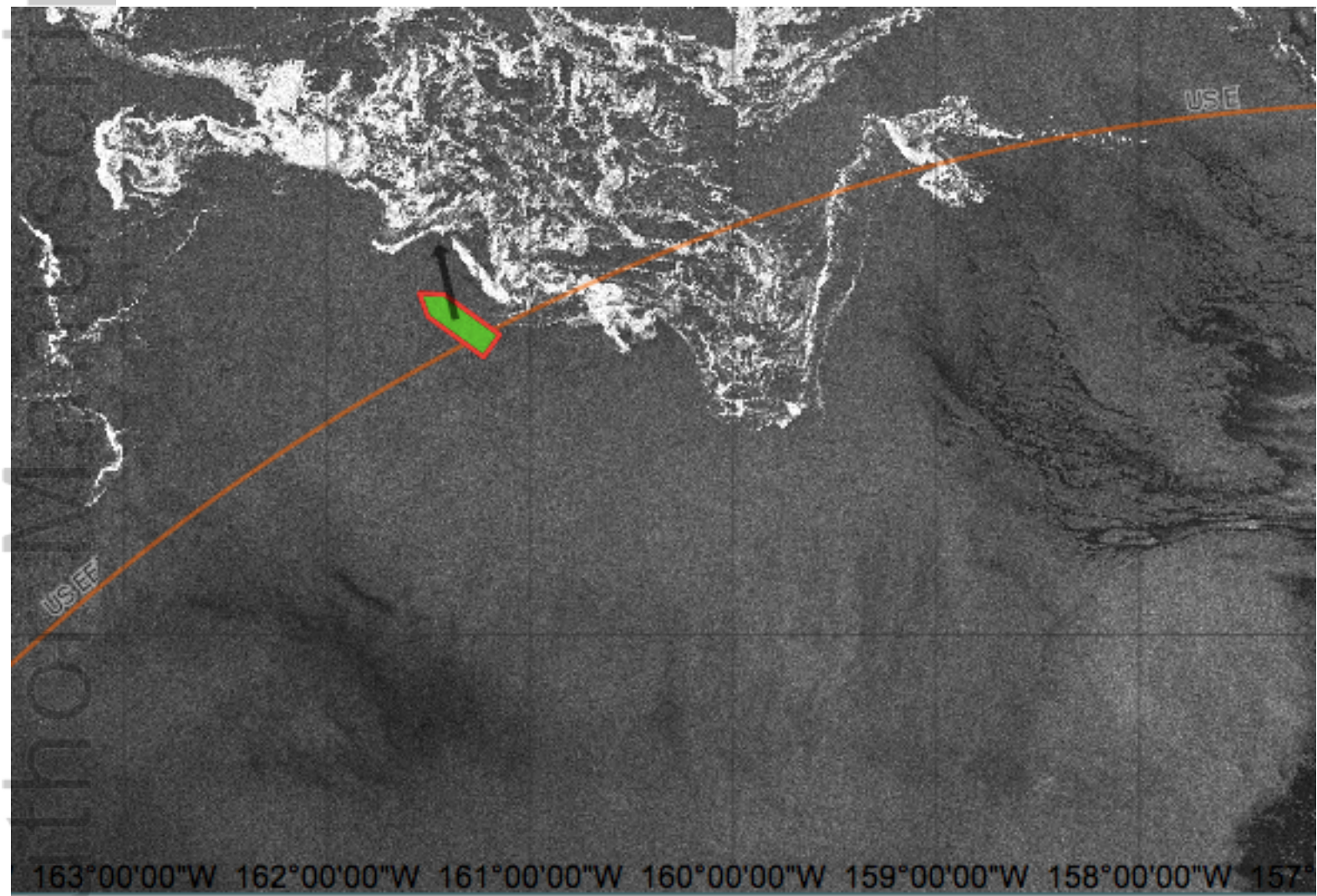


2018jc013766-f01-z-eps

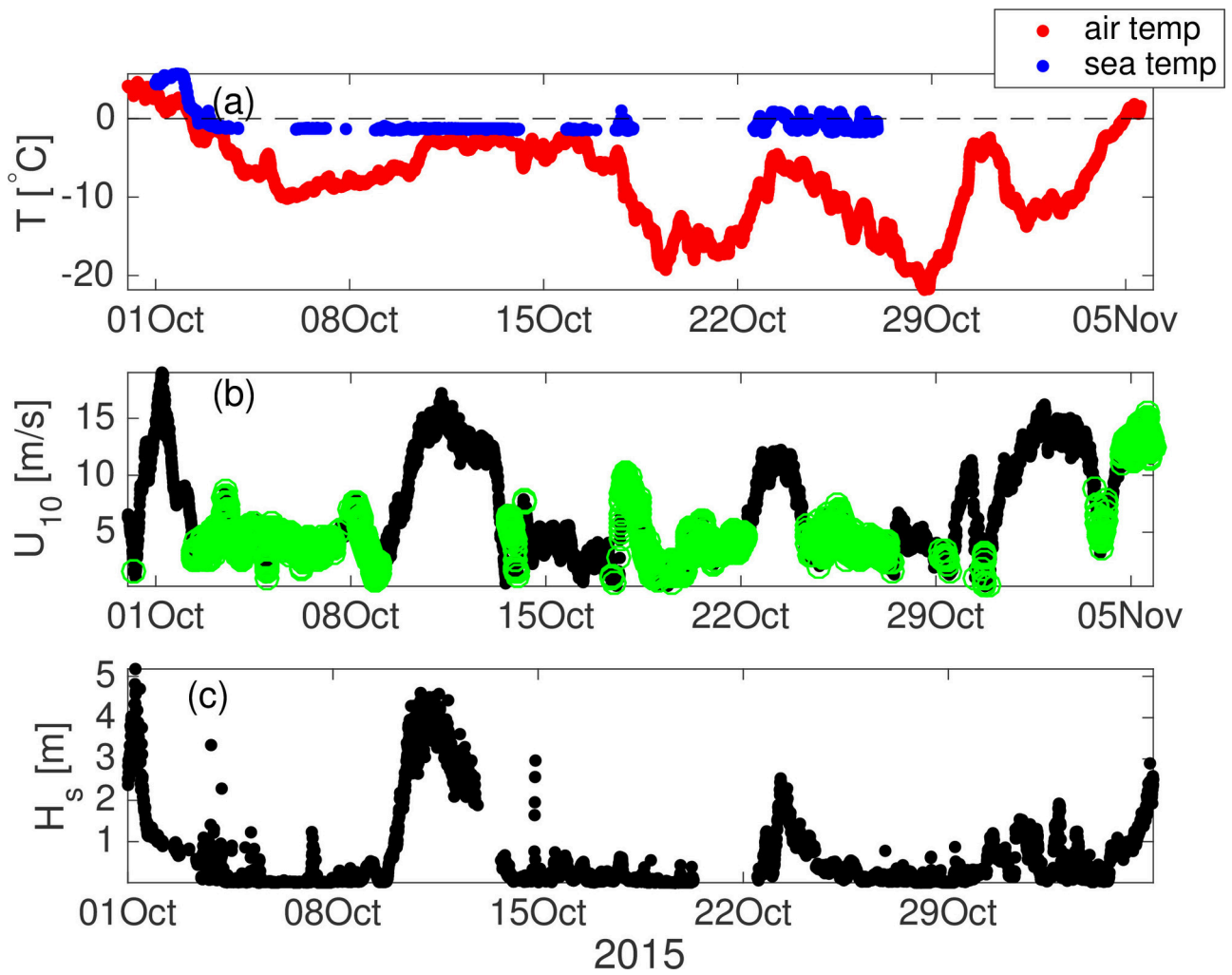
10-Nov-2015 00:00:00 UTC
WW3 sig. wave height (m) and mean wv. dir.



2018JC013766-f02-z-.png



2018JC013766-f03-z.png



2018jc013766-f04-z-.eps

Oct 10 2326 UTC

8.2 m/s /96°

$T_{s15} = -6.5^{\circ} \text{ C}$

$T_s = -1.3^{\circ} \text{ C}$

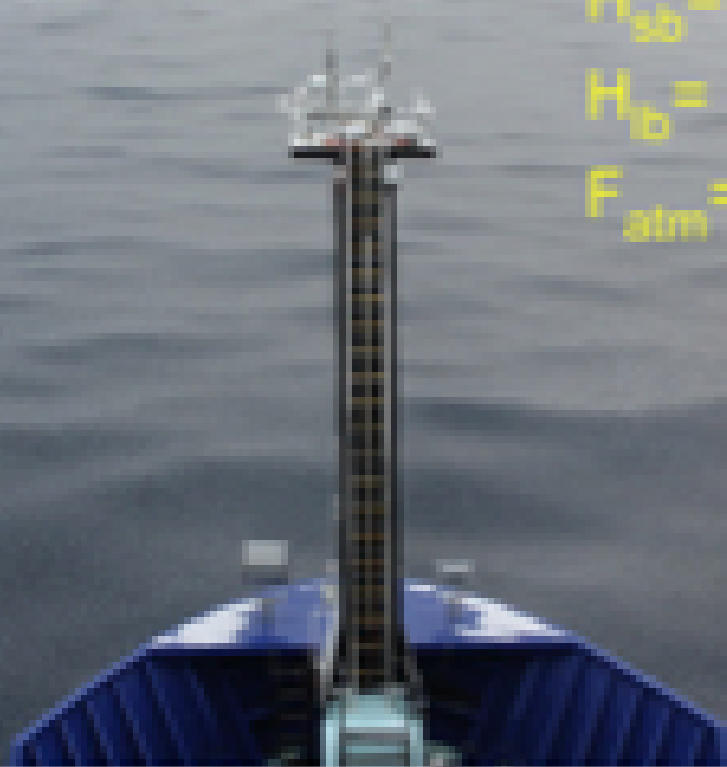
$SW_n = 29 \text{ W m}^{-2}$

$LW_n = -31 \text{ W m}^{-2}$

$H_{sb} = -65 \text{ w m}^{-2}$

$H_{10} = -49 \text{ W m}^{-2}$

$F_{atm} = -115 \text{ W m}^{-2}$



Oct 12 2228 UTC

14.0 m/s /114°

$T_{s15} = -2.8^{\circ} \text{ C}$

$T_s = -1.3^{\circ} \text{ C}$

$SW_n = 24 \text{ W m}^{-2}$

$LW_n = -13 \text{ W m}^{-2}$

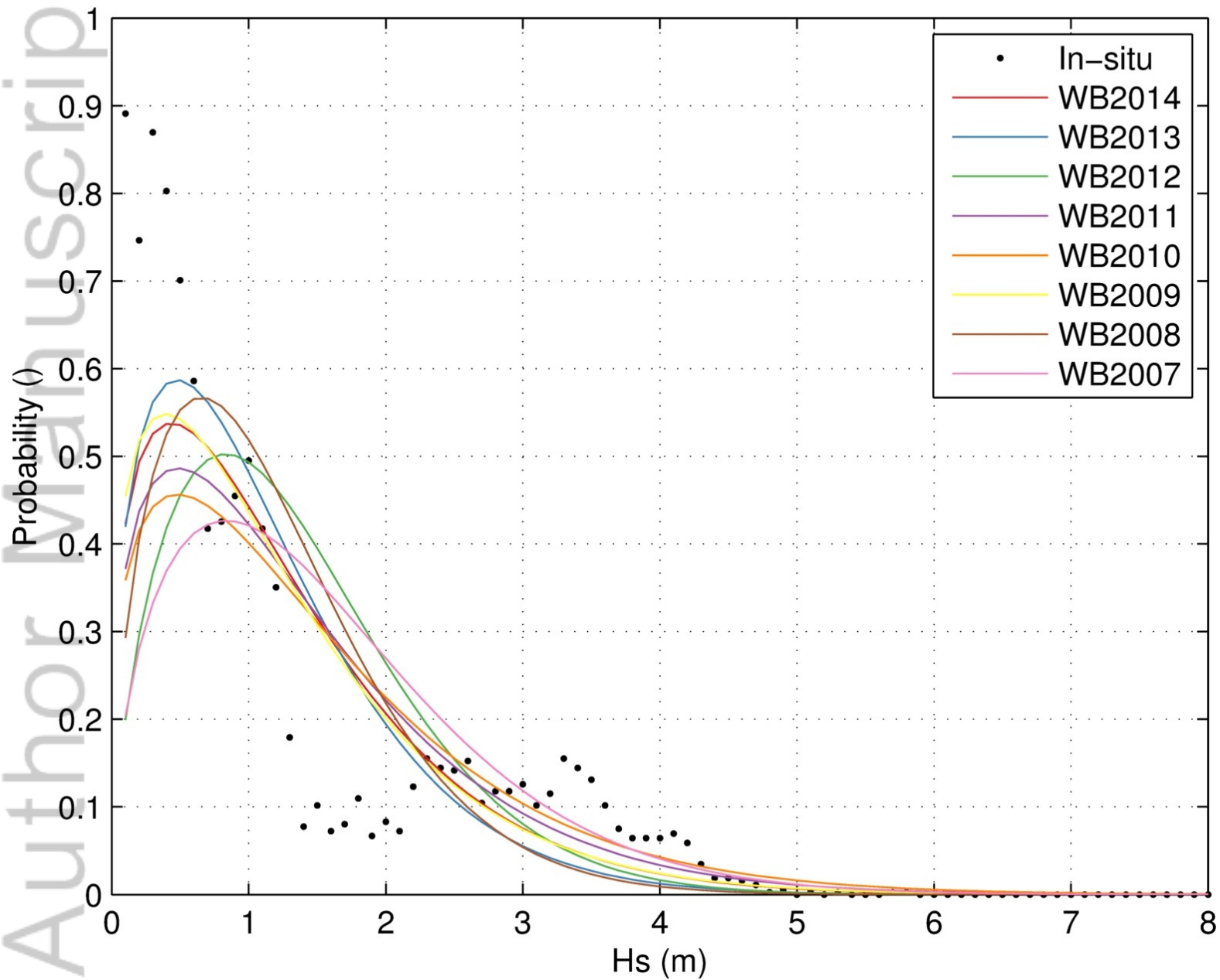
$H_{sb} = -26 \text{ w m}^{-2}$

$H_{10} = -44 \text{ W m}^{-2}$

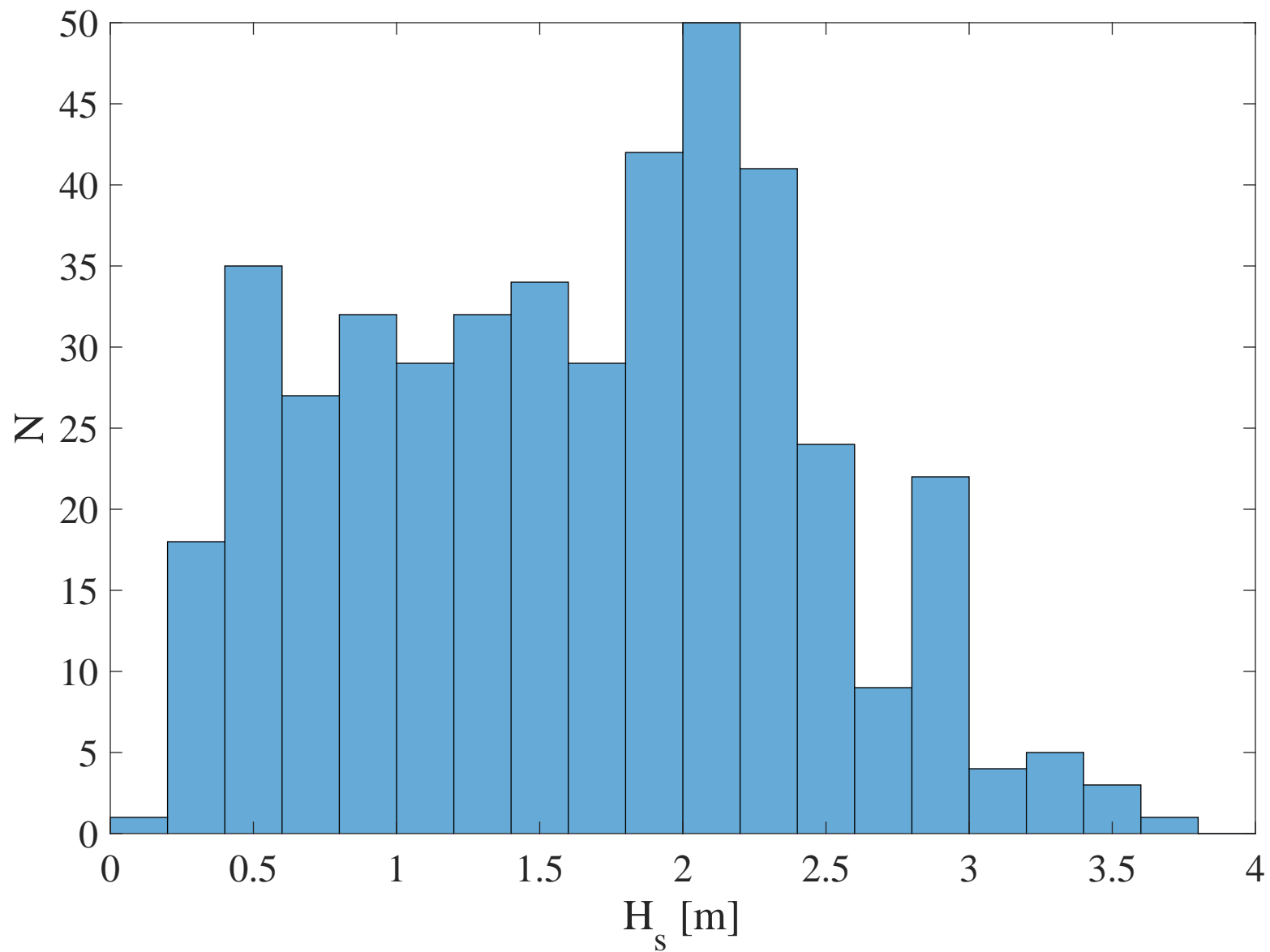
$F_{atm} = -59 \text{ W m}^{-2}$

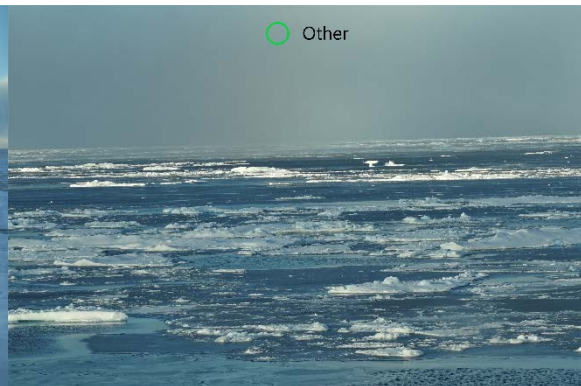
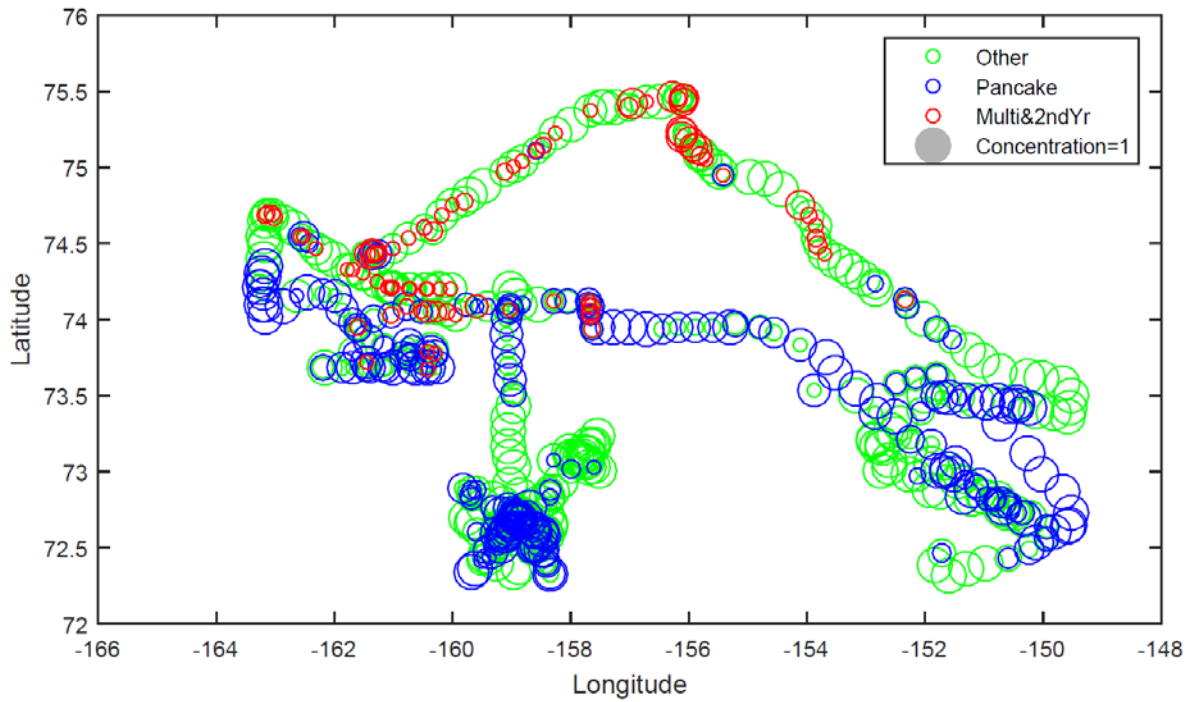


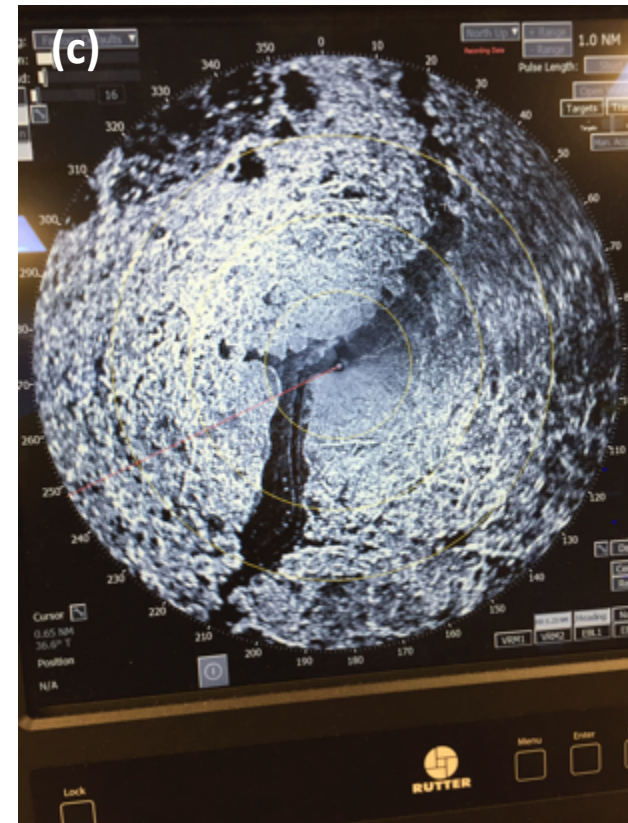
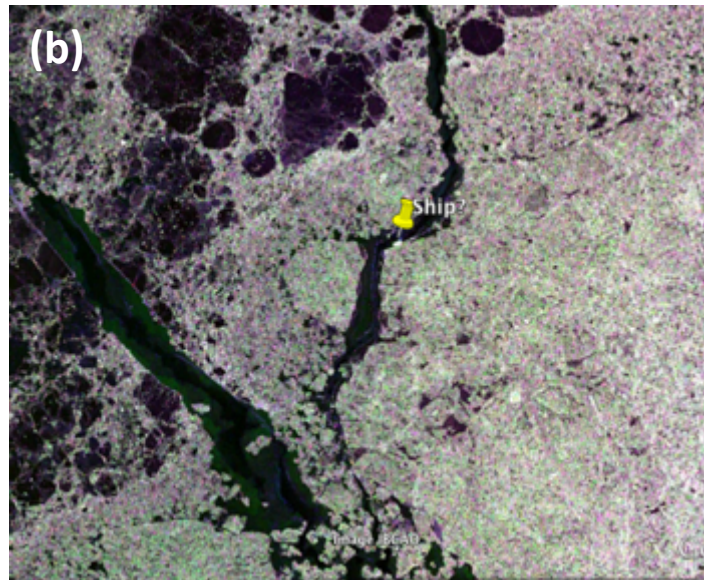
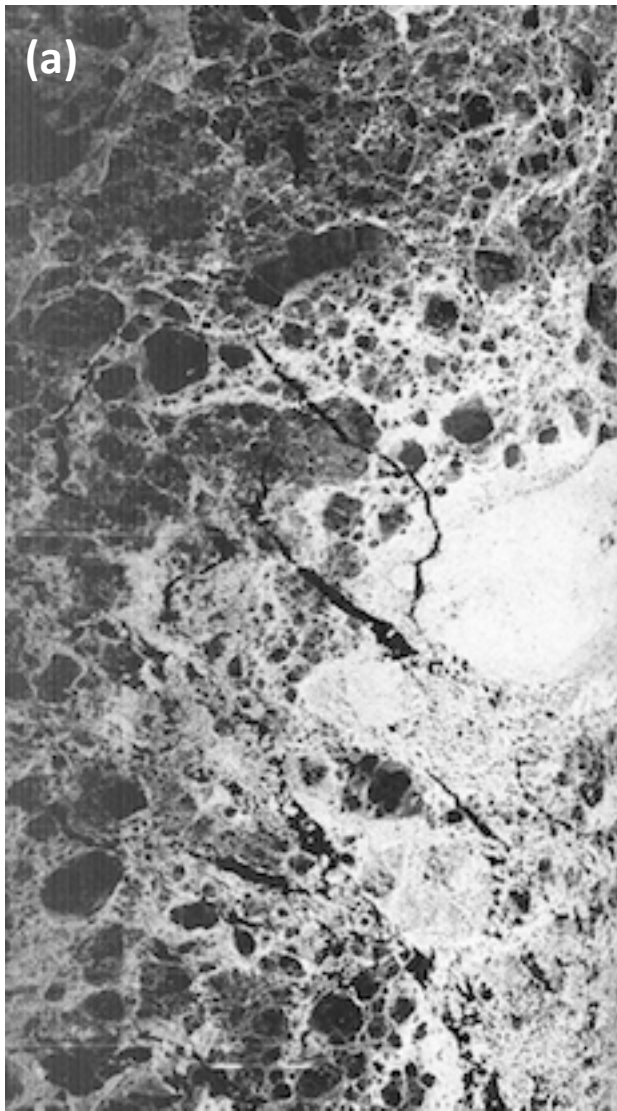
PDFs October: SeaState (2015) vs WW3 hindcast



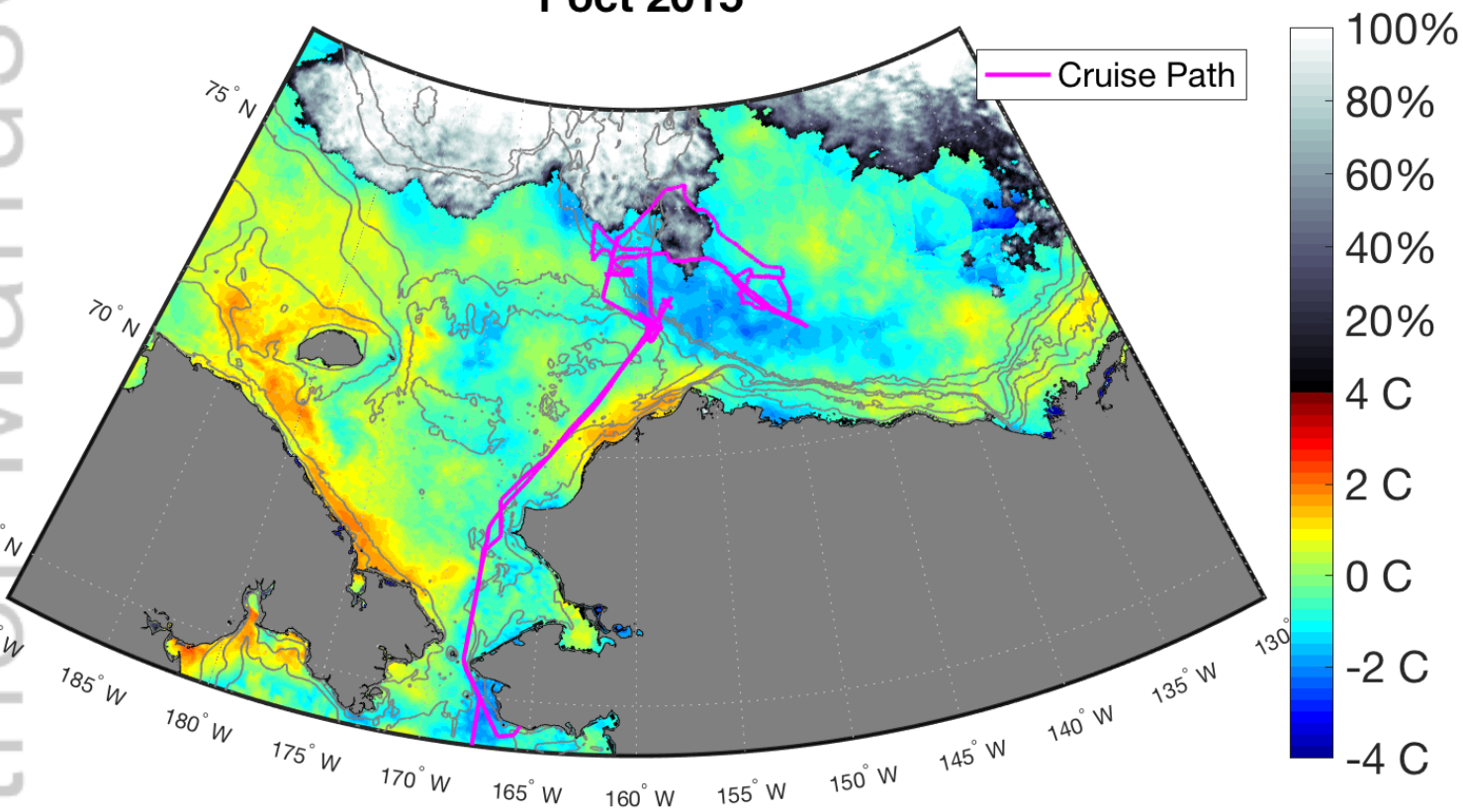
2018JC013766-f06-z-jpg





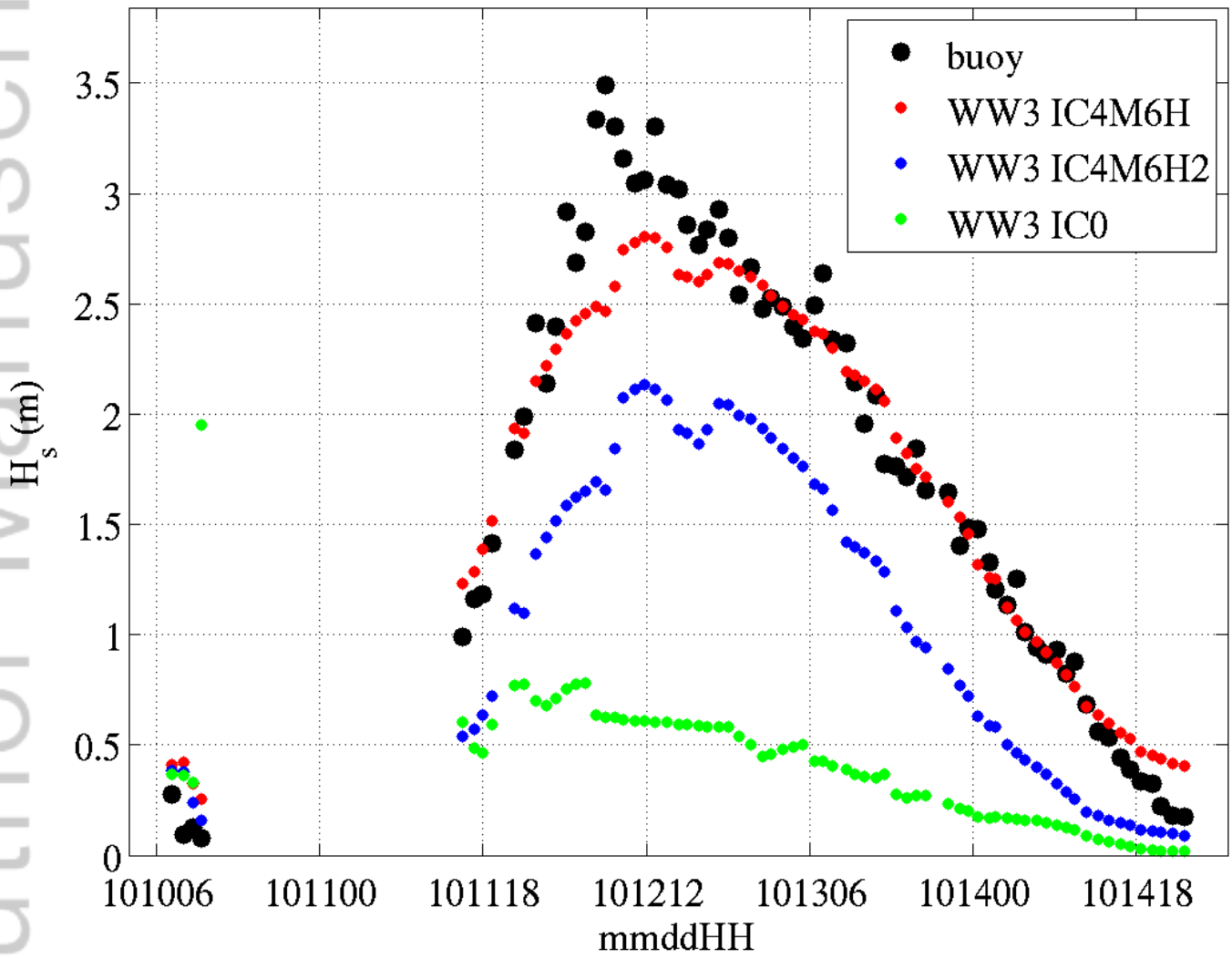


Sea ice concentration and sea surface temperature anomaly 1 oct 2015

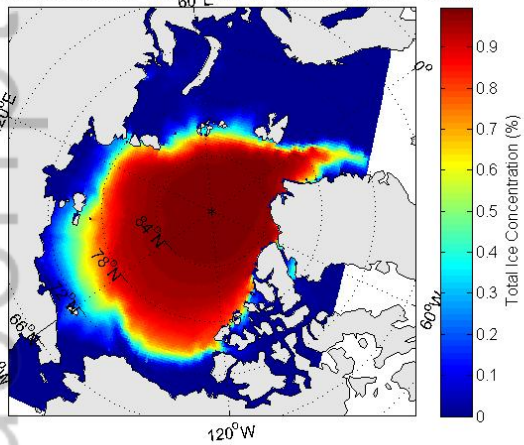


2018JC013766-f10-z-.png

NIWA2

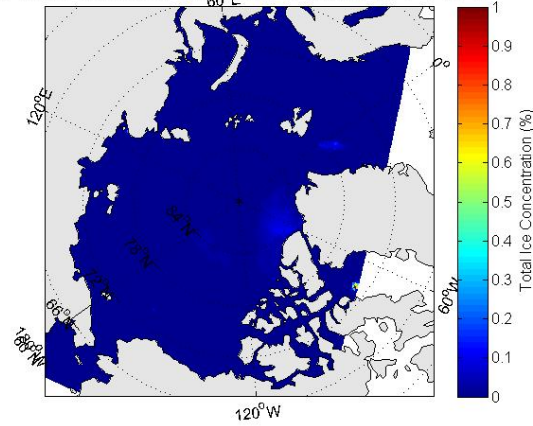


30 years mean ice coverage (Present 1970 - 1999)

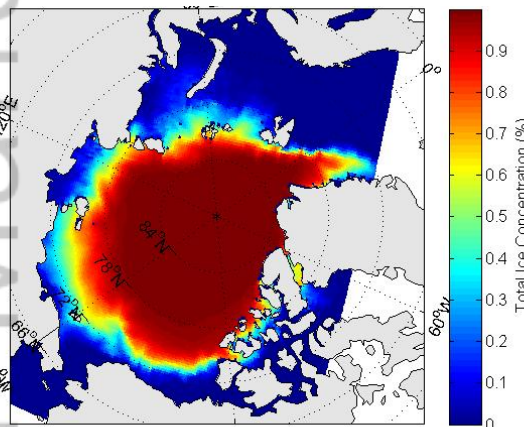


120°W

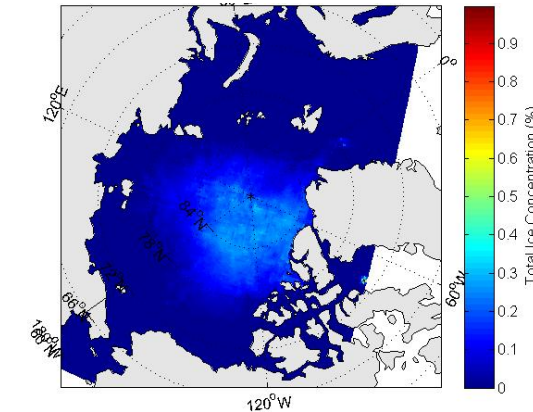
30 years mean ice coverage (Future 2070 - 2099)



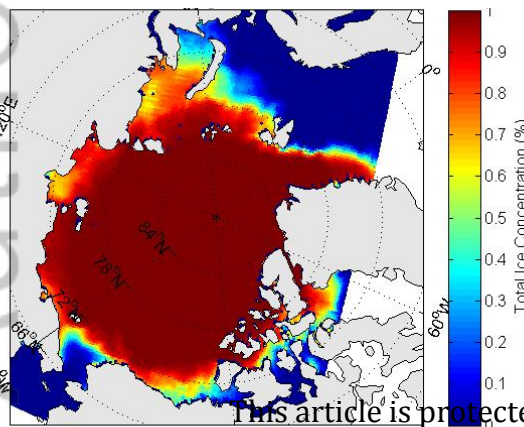
120°W



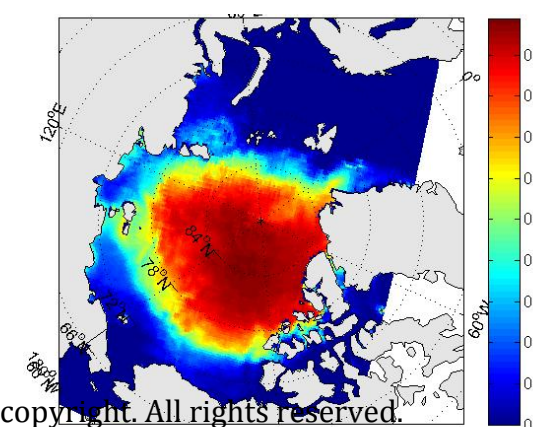
120°W



120°W



120°W



120°W

CIOM: A1B scenario

August

September

October



Minerva Access is the Institutional Repository of The University of Melbourne

Author/s:

Thomson, J; Ackley, S; Girard-Ardhuin, F; Ardhuin, F; Babanin, A; Boutin, G; Brozena, J; Cheng, S; Collins, C; Doble, M; Fairall, C; Guest, P; Gebhardt, C; Gemmrich, J; Graber, HC; Holt, B; Lehner, S; Lund, B; Meylan, MH; Maksym, T; Montiel, F; Perrie, W; Persson, O; Rainville, L; Rogers, WE; Shen, H; Shen, H; Squire, V; Stammerjohn, S; Stopa, J; Smith, MM; Sutherland, P; Wadhams, P

Title:

Overview of the Arctic Sea State and Boundary Layer Physics Program

Date:

2018-12-01

Citation:

Thomson, J., Ackley, S., Girard-Ardhuin, F., Ardhuin, F., Babanin, A., Boutin, G., Brozena, J., Cheng, S., Collins, C., Doble, M., Fairall, C., Guest, P., Gebhardt, C., Gemmrich, J., Graber, H. C., Holt, B., Lehner, S., Lund, B., Meylan, M. H. ,... Wadhams, P. (2018). Overview of the Arctic Sea State and Boundary Layer Physics Program. JOURNAL OF GEOPHYSICAL RESEARCH-OCEANS, 123 (12), pp.8674-8687. <https://doi.org/10.1002/2018JC013766>.

Persistent Link:

<http://hdl.handle.net/11343/284912>

File Description:

Accepted version